ALBERTA INNOVATES

CLEAN RESOURCES FINAL REPORT PACKAGE

Project proponents are required to submit a Final Report Package, consisting of a Final Public Report and a Final Financial Report. These reports are to be provided under separate cover at the conclusion of projects for review and approval by Alberta Innovates (AI) Clean Resources Division. Proponents will use the two templates that follow to report key results and outcomes achieved during the project and financial details. The information requested in the templates should be considered the minimum necessary to meet AI reporting requirements; proponents are highly encouraged to include other information that may provide additional value, including more detailed appendices. Proponents must work with the AI Project Advisor during preparation of the Final Report Package to ensure submissions are of the highest possible quality and thus reduce the time and effort necessary to address issues that may emerge through the review and approval process.

Final Public Report

The Final Public Report shall outline what the project achieved and provide conclusions and recommendations for further research inquiry or technology development, together with an overview of the performance of the project in terms of process, output, outcomes and impact measures. The report must delineate all project knowledge and/or technology developed and must be in sufficient detail to permit readers to use or adapt the results for research and analysis purposes and to understand how conclusions were arrived at. It is incumbent upon the proponent to ensure that the Final Public Report **is free of any confidential information or intellectual property requiring protection**. The Final Public Report will be released by Alberta Innovates after the confidentiality period has expired as described in the Investment Agreement.

Final Financial Report

The Final Financial Report shall provide complete and accurate accounting of all project expenditures and contributions over the life of the project pertaining to Alberta Innovates, the proponent, and any project partners. The Final Financial Report will not be publicly released.

Alberta Innovates is governed by FOIP. This means Alberta Innovates can be compelled to disclose the information received under this Application, or other information delivered to Alberta Innovates in relation to a Project, when an access request is made by anyone in the general public.

In the event an access request is received by Alberta Innovates, exceptions to disclosure within FOIP may apply. If an exception to disclosure applies, certain information may be withheld from disclosure. Applicants are encouraged to familiarize themselves with FOIP. Information regarding FOIP can be found at http://www.servicealberta.ca/foip/. Should you have any questions about the collection of this information, you may contact the Manager, Grants Administration Services at 780-450-5551.

ALBERTA INNOVATES

CLEAN RESOURCES FINAL PUBLIC REPORT TEMPLATE

1. PROJECT INFORMATION:

Project Title:	**A Multifaceted Graphene Quantum Dots derived from Asphaltenes for Energy and Biomedical Applications**
Alberta Innovates Project Number:	212201499
Submission Date:	March 18, 2024
Total Project Cost:	$392,158
Alberta Innovates Funding:	$200, 000
AI Project Advisor:	Paolo Bomben

2. APPLICANT INFORMATION:

Applicant (Organization):	**University of Calgary**
Address:	2500 University Drive NW
Applicant Representative Name:	Milana Trifkovic
Title:	Professor
Phone Number:	+1 (403) 220-8779
Email:	mtrifkov@ucalgary.ca

3. PROJECT PARTNERS

Please provide an acknowledgement statement for project partners, if appropriate.

RESPOND BELOW

Organization Name	Cash Funding	In-Kind Contribution	Committed?
Alberta Innovates	200000	0	Yes
University of Calgary	105158	87000	Yes

We are grateful to the University of Calgary for the cash funding and in-kind contribution. We also appreciate the university's commitment to the project.

A. EXECUTIVE SUMMARY

Provide a high-level description of the project, including the objective, key results, learnings, outcomes and benefits.

RESPOND BELOW

In this project we developed a technology to convert Alberta oilsands asphaltenes (AOA) to asphaltene-derived quantum dots (ACDs) which can serve as a platform technology for multiple applications in energy, environment and biomedical sectors.
The key goals of the project are:

(i) Development of asphaltene-derived quantum dots (ACDs) from Alberta oilsands asphaltenes.

(ii) Identifying the composition of the asphaltene oxide intermediate in the ACDs synthesis process.

(iii) Validating ACDs use as nanotracers for cancer imaging and photothermal therapy at the lab scale.

(iv) Validating ACDs as nanotracers for fracking fluids, nanoadditives for water-based lubricants, nanoadditives for enhancing thermal conductivity, emulsion stabilizers at ultra-low loadings.

(v) Performing preliminary economic analysis of ACDs in both energy and biomedicine sectors.

High yield asphaltene-derived quantum dots (ACDs) with super-hydrophilicity have been successfully synthesized from Alberta oilsands asphaltenes using two different synthesis routes in our lab and extensively characterized. With exception of validating fracking fluid nanotracers in the simulated environment, we have validated the effectiveness of ACDs in all other

applications in the simulated environment.

The successful implementation of this technology or use of the knowledge generated could result in:

(a) Providing a high-value market for Alberta's natural resources.

(b) Reductions in greenhouse gases emission.

(c) Diversifying Alberta's economy that is hitherto oil-production dependent.

(d) Improving the health and well-being of Alberta cancer patients.

B. INTRODUCTION

Please provide a narrative introducing the project using the following sub-headings.

- **Sector introduction:** Include a high-level discussion of the sector or area that the project contributes to and provide any relevant background information or context for the project.
- **Knowledge or Technology Gaps:** Explain the knowledge or technology gap that is being addressed along with the context and scope of the technical problem.

RESPOND BELOW

Sector introduction:

Alberta oilsands asphaltenes (AOAs) which necessitates the development of a technology for their conversion to value added materials. Herein, we propose a new aspect of useful conversion of AOAs to asphaltene-derived carbon dots (ACDs) that can serve metal-ion nanosensors, water-based lubricant additives, antifreeze thermal conductivity enhancers, oil-in-water high interface Pickering emulsion stabilizers, holographic sensors component, subsurface fluid tracers and cancer imaging and therapeutic agent. This project therefore contributes to energy, environment and biomedical (cancer imaging and therapy) sectors.

Geothermal energy, metal detection, emulsion stabilization, fracking fluids, and cancer diagnostics markets account for about $98 billion, $4.1 billion, $1.8 billion, $32.4 billion, and $17.2 billion in recent global markets. We expect that the success of this innovation would revolutionize these industries, thus giving us envisaged access to ~5% of the market.

In biomedicine, cancer accounts for about 10 million deaths globally. Early detection is one of the most effective ways to reduce mortality. Photothermal and magnetic resonance imaging are among the widely researched tumor imaging modalities. Based on the intrinsic properties of ACDs, they can serve as a nanoprobe for tumor imaging by photothermal or magnetic resonance imaging. This can promote early cancer detection and diagnosis which are key to proper cancer treatment.

Knowledge or Technology Gaps:

A major drawback to asphaltenes technology development is the source-dependent variation of asphaltenes composition. Consequently, synthesis routes reported so far in the literature for converting asphaltenes to ACDs do not show translation of such technologies to different sources of asphaltenes. Conventional synthesis of ACDs from asphaltenes or their graphene analogues operate at high temperature and pressure.

Hydrophilicity of such ACDs is poor and further jeopardized after drying as re-dispersion in water becomes challenging. These are complicated by the necessary post-synthesis filtration step to remove byproducts, resulting in low mass yield of the recovered ACDs. Moreover, there is yet no technology that showcase the isolation of large size nanoparticles (asphaltene oxide) in a single synthesis process enroute the generation of ACDs from asphaltenes.

C. PROJECT DESCRIPTION

Please provide a narrative describing the project using the following sub-headings.

- **Knowledge or Technology Description:** Include a discussion of the project objectives.
- **Updates to Project Objectives:** Describe any changes that have occurred compared to the original objectives of the project.
- **Performance Metrics:** Discuss the project specific metrics that will be used to measure the success of the project.

RESPOND BELOW

Knowledge or Technology Description:

The technology developed in this project has enabled the consistent synthesis of ACDs of very similar properties from different sources of asphaltenes, thus evading the source-dependent asphaltenes composition variation. We support this claim by the extensive characterization of the derived ACDs in terms of the hydrophilicity, morphology, size, surface charge, thermal stability, surface functionality, defect states, crystallinity, light absorption, and photoluminescence. Asphaltene oxide isolated during the synthesis process using various sources of asphaltenes also exhibit indistinguishable properties. Our technology also affords regular synthesis of the ACDs and asphaltene oxide at lower temperature than the conventional, without need for external pressure. It is interesting to note that even after extensive oven drying, the ACDs and asphaltene oxide obtained from our technology exhibit excellent re-dispersibility without external impetus of water-bath ultrasonication. Our technology involves a facile but extensive oxidation of asphaltenes to reasonable extents that side-step the conventional need for post-synthesis filtration to remove by-products. This has enabled us to obtain mass yield of the ACDs and asphaltene oxide that are well above those available in literature. The ACDs synthesized from out technology was utilized in various unrelated fields viz: First, the impressively hydrophilic ACDs with variety of surface functionality were leveraged to complex with iron and manganese to prepare Magnetic Resonance Imaging (MRI) contrast agents to meet the pre-requisite for application as hydraulic fluid tracers. Second, the impressive hydrophilicity of the ACDs, which is a highly sought-after property of nanomaterials for biomedical application, position them for potential biomedical application. And this has been substantiated in our laboratory. Third, the impressive hydrophilicity of the ACDs was also leveraged in preparing water-based nanofluids that guarantee re-dispersibility of ACD particles to afford substantial friction reduction between steel/steel interfaces. Fourth, the ACDs nanofluids are good thermal conductivity enhancers in water, ethylene glycol and antifreeze (car radiator coolant). Fifth, the ACDs are further explored as high interface

Pickering emulsion stabilizers where unprecedented low loading of the ACDs stabilize high oil volume fraction emulsion with considerable long-term stability and flowable properties that offer using the ACDs-stabilized emulsions in 3D printing. Sixth, the ACDs show appreciable dispersibility in various polymers (e.g., chitosan, cellulose, PEO) and thus used alongside polyvinyl alcohol to prepare holographic sensing material.

Updates to Project Objectives:

We have not changed the project objectives from the original. The first two objectives of the project (1) development of asphaltene-derived quantum dots (ACDs) from Alberta oilsands asphaltenes, and (2) identifying the composition of the asphaltene oxide intermediate in the ACDs synthesis process, have been carried out extensively and completed. Regarding the composition identification of the ACDs and asphaltene oxide, we conducted extensive analysis using transmission electron microscopy for determining morphology; confocal microscopy to visualize water dispersibility; X-ray diffraction spectroscopy for investigating crystal property; dynamic light scattering to measure particle size and zeta potential (surface charge); inductively couple plasma-optical emission spectroscopy to determine elemental composition; X-ray photoelectron spectroscopy for measuring chemical and electronic states of atoms; Fourier transform infrared spectroscopy and X-ray photoelectron spectroscopy to ascertain functional groups; Raman spectroscopy to understand the defect states; ultraviolet-visible spectroscopy to determine absorption wavelength; and fluorescence spectroscopy for the determination of optical properties. Their utilization as tracers was initiated, and the first experiments investigated their complexation capability with iron and manganese was conducted and proton MRI relaxivities have been obtained. The application in tumor imaging and therapy has now been completed. Furthermore, the ACDs are applied as water-based lubricant additives, metal-ion detectors, antifreeze thermal conductivity enhancers, high interface Pickering emulsion stabilizers, in vivo tumor MRI probe, and as a component of holographic sensing composite.

Performance Metrics:

The success of this project will be determined at the end of the project by the following metrics:

(a) Synthesizing ACDs up to 20g/day.

(b) Obtaining the ACDs at sizes below 20 nm.

(c) Obtaining up to 5 different colors of the ACDs.

(d) Achieving less than 5% retention of the ACDs in core flood apparatus.

(e) Substantiating cellular uptake of the ACDs by tumor cells, establishing their resistance to photobleaching, achieving tumor photothermal therapy, and enabling tumor imaging up to 30 min post injection.

(f) Obtaining asphaltene oxide as intermediate product during ACDs synthesis and applying them as a useful value-added material.

D. METHODOLOGY

Please provide a narrative describing the methodology and facilities that were used to execute and complete the project. Use subheadings as appropriate.

RESPOND BELOW

Syntheses of ACDs and asphaltene oxide

ACDs and asphaltene oxide syntheses proceeded by oxidation of the asphaltenes precursor. Asphaltene oxide could easily be obtained as an isolable intermediate during the oxidation process. Thereafter, the mixture (containing either asphaltenes oxide or ACDs) was centrifuged at 3000 rpm for 10 min and this process was repeated three times to remove the acid components. The product (either asphaltenes oxide or ACDs) was further purified by dialysis in a dialysis membrane (molecular weight cut off = 3500 Da) against DI water for 2 days with daily change of water. The super hydrophilic ACDs or asphaltene oxide were then obtained as a fine black powder after vacuum drying for 48 h at 50°C.

Preparation of ACD-metal complex for hydraulic fracking with MRI

ACD-metal ion complexes were prepared using various concentrations of Fe^{3+} and Mn^{2+} in ACD, and their magnetic resonance imaging (MRI) contrast-enhancing capability was assessed. T_2 MRI relaxivities were obtained for pristine ACDs, ACDs-Fe complex and ACD-Mn complex. This was conducted to understand their capability for hydraulic fracking tracing with the MRI technique.

Preparation of ACDs-stabilized high interface Pickering emulsions

High interface Pickering emulsions (HIPEs) were prepared by adding the oil phase to the ACDs suspension in water. To ensure a homogeneous blend and the formation of a stable emulsion, this mixture was subjected to a thorough homogenization.

Preparation of ACDs/photopolymer nanocomposite holography recording material

Doping the photopolymer solution with the ACDs was done by solution mixing. The photopolymer solution was spread evenly on a glass substrate. The coated glass substrate was placed on a flat surface and allowed to dry in the dark.

Characterization of the ACDs and asphaltene oxide

The morphology of the ACDs and asphaltene oxide was investigated on a JEOL JEM-ARM200cF transmission electron microscope (TEM), which was operated at a 200 kV accelerating voltage. The microscope was equipped with a cold field-emission gun and a probe spherical aberration corrector. Dynamic light scattering (DLS) and zeta potential distribution of the ACDs and asphaltene oxide were measured on a Zetasizer Nanoseries device (Nano-ZS, Malvern Instruments, Britain) to determine the sizes and surface charges of the nanoparticles, respectively. The functional groups in pristine asphaltenes and ACDs and asphaltene oxide were determined by X-ray photoelectron spectroscopy (XPS) using Kratos Axis Ultra XPS spectrometer (Kratos Analytical, USA), and Fourier transform infrared (FT-IR) spectroscopy conducted on an Agilent Cary 630 FTIR Spectrometer (Agilent Instruments, USA). Dispersibility of the ACDs, asphaltene oxide and ACDs-derived nanofluids for friction reduction studies was assessed by confocal microscopy on a Leica DMi8 (Leica Microsystems, USA) at 405 nm excitation wavelength. Elemental analysis of pristine asphaltenes, ACDs, and

asphaltene oxide was conducted on an Agilent 8900 inductively coupled plasma mass spectrometer (Agilent Instruments, USA).

Cell culture and in vitro cytotoxicity assay

Mouse breast cancer (4T1) cell lines were cultured in RPMI-1640 medium supplemented with 10% FBS, 100 mg/mL streptomycin (Keygene) and 100 unit/mL penicillin, at 37°C in a 5% CO2 humidified atmosphere. The in vitro cytotoxicity of the ACDs was determined by MTT assay. Typically, 100 µL 4T1 cells were separately seeded into 96-well culture plates at 1×10^5 cells per mL and cultured for 24 h at 37°C in 5% CO_2. The cells were then washed thrice with phosphate-buffered saline (PBS, pH=7.4) and subsequently incubated alongside different concentrations (20, 40, 60, 80, and 100 µg/mL) of ACDs for 24 h. Thereafter, 10 µL of 5 mg/mL MTT solution was added to each well and further incubated at 37°C in 5% CO_2 for 4 h. Then, the growth medium was removed, followed by the addition of 100 µL DMSO to each well to dissolve the formazan crystals. The cells were co-incubated with the materials and MTT solution for another 30 min. Thereafter, absorbance of the resulting solutions in the wells was measured at 490 nm using a microplate reader (iMark 168-1130, Bio-rad, USA). The control group contained 4T1 cells and culture medium without the ACDs.

In vitro cancer PTT

To investigate the therapeutic ability of the ACDs, 100 µL of 4T1 cells (1×10^5 per mL) were separately incubated in 96-well plates for 24 h in RPMI-1640 medium. Then, 100 µL of fresh media or 100 µL media containing various concentrations (10, 20, 30, 40, and 50 µg/mL) of the ACDs were used to replace the old cell culture medium and incubated for another 24 h. After washing with PBS several times, 100 µL of fresh cell culture medium was added into the cells. Subsequently, the cells were irradiated for 5 min with an 808 nm laser operated at 1.0 W/cm^2. To study the effect of optical density on therapeutic efficacies, the concentration of the ACDs was kept constant at 50 µg/mL in freshly prepared 96-well plates with 4T1 cells (1×10^5 per mL), while laser power density was varied (0.5, 1.0, 1.5, and 2.0 W/cm^2). Absorbance of the resulting solutions in each well was measured at 490 nm with the microplate reader.

In vivo biocompatibility assay

To evaluate the biocompatibility of the ACDs in vivo, nude mice were divided into two groups (n=5). The first group was intravenously injected with 200 µL of 2 mg/mL ACDs, while the second group was intravenously injected with 200 µL PBS (pH=7.4) as control. The mice were observed up to 24 hours post-injection.

In vivo cancer photothermal imaging and PTT

The imaging and therapeutic experiments were performed to understand the capability of the ACDs for cancer photothermal imaging and therapy. Typically, PBS as control, and ACDs were injected into 4T1 tumor-bearing mice. Photothermal imaging was conducted with near infrared laser irradiation of the tumor region. PTT of the mice was then observed for a period of 15 days post-irradiation. The mice were randomly divided into two groups (n=5): (1) PBS + 808 nm laser group, and (2) ACDs + 808 nm laser group. The day of laser exposure was set as day 0. Body weights and tumor volumes were recorded over the 15-day observation period.

Phantom MRI with ACD-Fe complex

The magnetic resonance phantom studies were carried out on a 9.4 T scanner (Brucker Biospec 94/20, USA). T_2-weighted images of different concentrations of free Fe^{3+} (control) and ACD-Fe complex were obtained. Then, transverse (r_2) relaxivities of free Fe^{3+} (control) and ACD-Fe complex were determined as slopes of the plots of the inverse relaxation times ($1/T_2$) against Fe^{3+} concentration.

In vivo tumor MRI

For the in vivo imaging, the nude mice were anesthetized by the intraperitoneal injection of 50 µL sodium pentobarbital 15 min before imaging. Thereafter, the mice were injected with free Fe^{3+} and ACD-Fe complex. The MR images of the whole mice were acquired pre-injection and various times post-injection on the 0.5 T Mice MRI Research System.

Tribological Assessment

Tribological measurements were done using a rotational shear rheometer (MCR 302, Anton Paar, Austria) equipped with a tribology unit (T-PTD 200, Anton Paar, Austria) at a controlled temperature of 25±0.01°C. A steel sphere (100Cr6, 12.7 mm diameter) was rotated on the surfaces of three austenitic chromium-nickel stainless steel plates (AISI 304) with a roughness average (Ra) of 0.2 µm. The steel plates were fully submerged in the sample. A normal force of FN = 8.47 N was applied to the sample set and maintained constant throughout the experiment; this resulted in a tribological normal load FN,tribo = FN/3 cos(45°) = 4 N acting on each plate surface. The steel ball rotated with a speed n, from which the sliding speed vs = 2πnR sin(45°/60) was calculated. The rheometer maintained the speed by applying a torque M from which the frictional force FF = M/3R sin(45°) was calculated. The friction factor was therefore defined as µ = FF/FN,tribo. For the Stribeck curves, the sliding velocity was swept at least five times to ensure a steady state friction response; the reported friction curves represent the average of the last three sweeps to minimize the impact of run-in effects. Different loadings of the ACDs in water (0.2, 0.5, 1.0, 2.0, 4.0, 6.0, and 8.0 wt.%) were evaluated and DI water was used as control.

For the time-dependent tribological test, a constant sliding velocity of vs = 2 mm s^{-1} was applied on the various loadings of ACDs for 1 h at the mixed region of the Stribeck curve to monitor the time-dependent behavior of the samples. At this speed, a fluid film thickness of 4.63 nm was estimated for a water viscosity of 0.89 mPa.s, which translates to a shear rate of 4.32×10^5 1/s. The thickness of the lubricating film was calculated using the Nijenbanning and Moes equation, which was applied using an online calculator. The balls used in experiments had a 12.7 mm diameter, the applied normal force was 4 N, and the sliding velocity ranged was 2 mm/s. We used the elastic modulus for steel of 200 GPa, the Poisson ratio of 0.3 47. With a viscosity of water at 25°C of 0.89 mPa.s, which then yields a film thickness of 4.63 nm at a sliding speed of 2 mm/s, which translates to a shear rate of 4.32×10^5 1/s. Tribological assessment of various loadings of commercial 5 and 20 nm silica nanoparticles in water (0.2, 1.0, 4.0, and 8.0 wt.%) were conducted under the same conditions as with the ACDs nanofluids. DI water was also used as control.

Wear Scar Surface Analysis

After each tribology test, the steel plates were adequately washed with isopropyl alcohol solvent to remove any debris on wear scar regions of the steel plates. The wear scar surfaces, and wear scar diameter of the steel plates were analyzed using scanning electron microscopy (SEM) and energy dispersive X-ray spectroscopy (EDS) (Quanta FEG-250, FEI Oregon, USA). 3D surface mapping of the plates was obtained on a Physical Stylus Profilometer (Bruker DektakXT, USA).

Rheological Evaluation

The steady shear viscosity of the lubricant nanofluids was measured using a rotational shear rheometer (MCR 302, Anton Paar, Austria) equipped with a cone-and-plate geometry (50 mm diameter, 1° cone angle) at a controlled temperature of 25±0.01°C. Different loadings of the ACDs in DI water and the 5 and 20 nm silica nanofluids were evaluated before and after 1 h of constant shearing at a shear rate of 4.32×10^5 1/s (DI water was used as control).

E. PROJECT RESULTS

Please provide a narrative describing the key results using the project's milestones as sub-headings.

- Describe the importance of the key results.
- Include a discussion of the project specific metrics and variances between expected and actual performance.

RESPOND BELOW

Cost-effective synthesis route for converting asphaltenes to asphaltene-derived quantum dots (ACDs)

This process has been successfully achieved and even extended to showcase the robustness of our synthesis strategy that enables development of the ACDs from various sources of asphaltenes. We have established successful color tunability of the ACDs between orange and blue (Figure 1a). Furthermore, we have synthesized hydrophobic ACDs to complement the hydrophilic ACDs in hydraulic fracking tracing (Figure 1b). The hydrophobic ACDs show high affinity for the organic phase in a toluene–water solvent mixture and are expected to bind to oil components in underground wells to enable detecting oil-containing layers in the horizontal fracking regions.

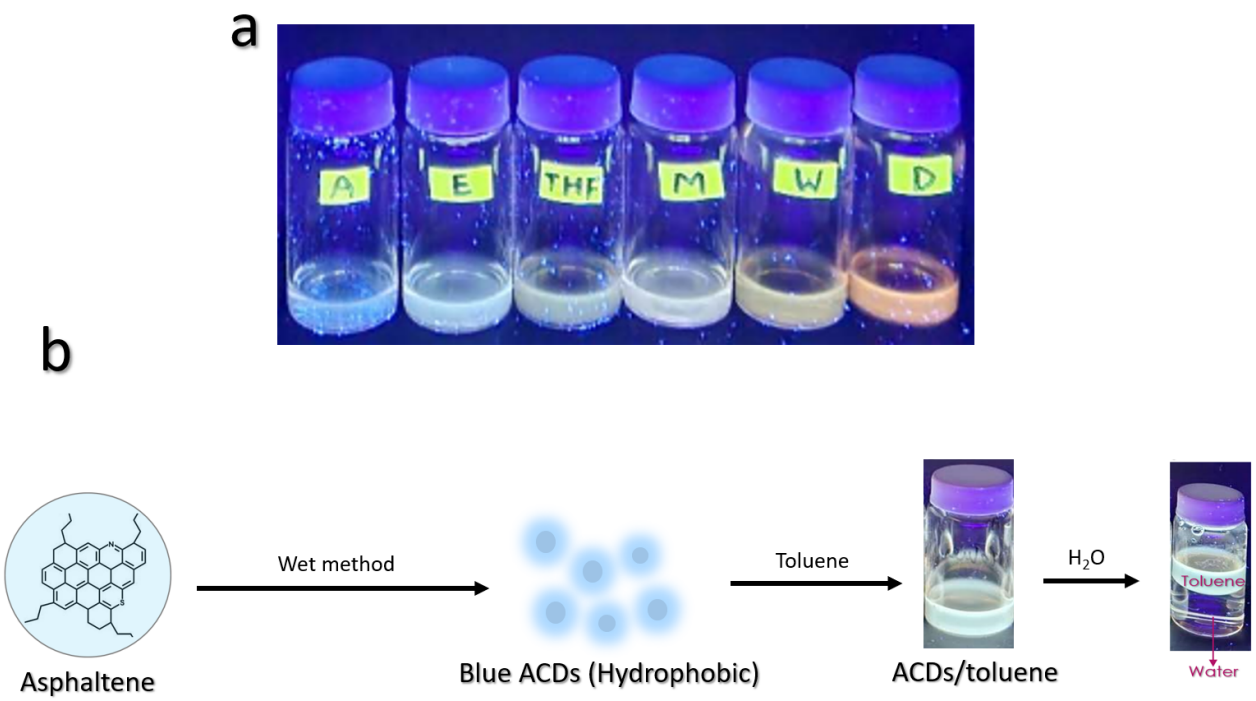

Figure 1: (a) The color tunability of the hydrophilic ACDs.
(b) Synthesis of hydrophobic ACDs and their interactions with toluene and water, showing high affinity for the organic (toluene) phase.

Characterization of the derived ACDs: We have extensively characterized the ACDs. Specifically, the hydrophilicity, morphology, size, surface charge, surface functionality, and contact angle of the ACDs are the major properties we have determined. The morphology, size, and zeta potential of asphaltene oxide (AO) and hydrophilic ACDs synthesized from two sources of asphaltenes are shown in Figure 2.

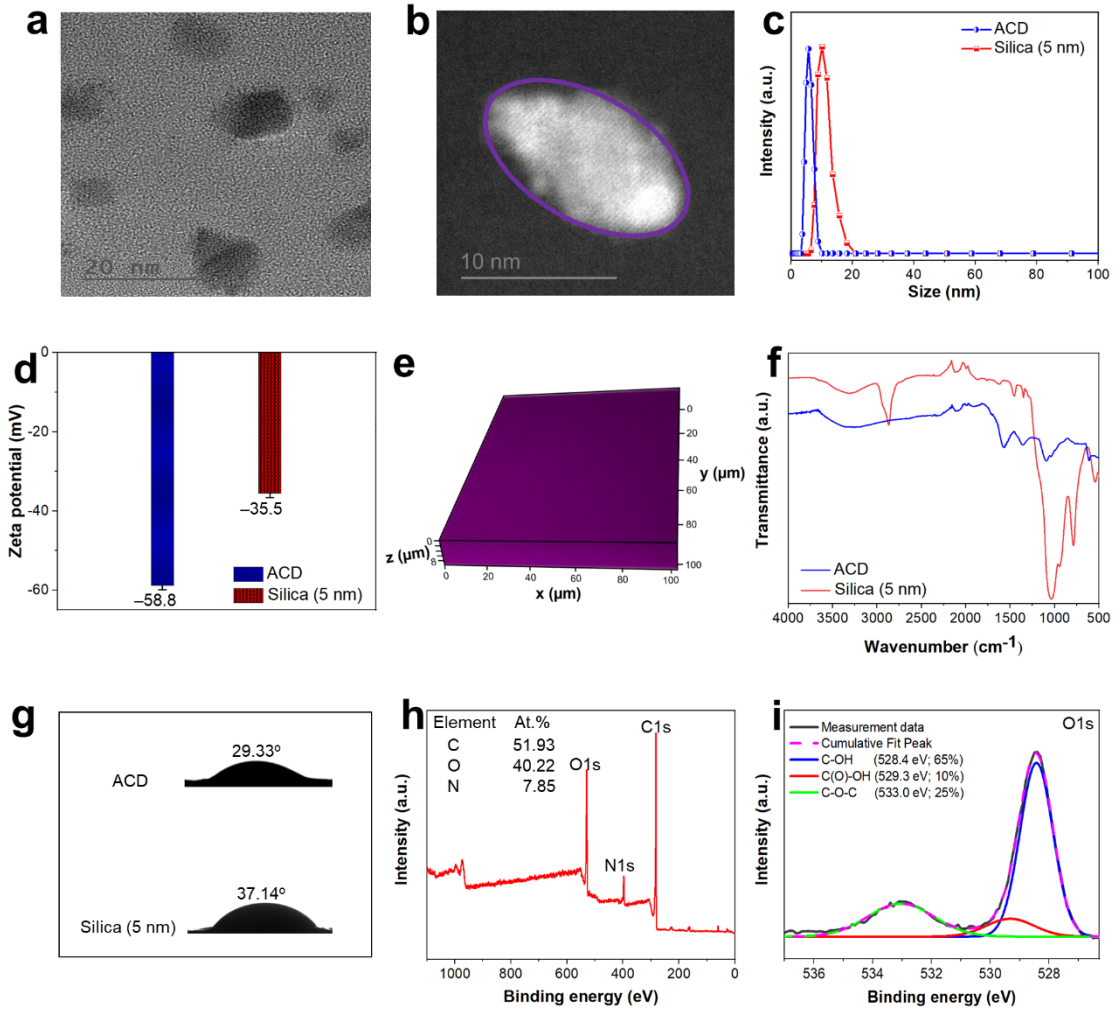

Figure 2. Physicochemical Characterization of ACDs. (a) TEM and (b) S/TEM images of the ACDs. (c) Size and (d) zeta potentials of the ACDs and 5 nm silica nanoparticles dispersion in water. (e) 3D confocal microscopic image of 275 mg mL-1 ACDs dispersion in water. (f) FT-IR spectra and (g) contact angles of the ACDs and 5 nm silica nanoparticles. (h) XPS full survey and (i) O1s XPS scans of the ACDs.

It is noteworthy that ACDs synthesized from both asphaltene sources generally exhibit similar properties. The TEM images reveal oval shape of the ACDs with sizes below 10 nm in each case. This was confirmed in the dynamic light scattering image (size) where ACDs size of 5.28 was obtained. As the ACDs are synthesized by oxidation of asphaltenes, oxygen- and nitrogen-containing groups are present on the surfaces of the ACDs and asphaltenes, which are responsible for the negative zeta potentials. The surface charge of the ACDs is –58 mV. Such high negative charge has yet to be achieved for asphaltene-derived ACDs available in the literature, which also outperforms that of commercial 5 nm silica nanoparticles used as a comparison. This

points to the uniqueness of our technology that ensures extensive oxidation of the parent asphaltenes to generate the ACDs. Further testing of the asphaltene oxide and hydrophilic ACDs from the two sources of asphaltenes have also been conducted. Figure 3 shows the properties of asphaltene oxide (AO).

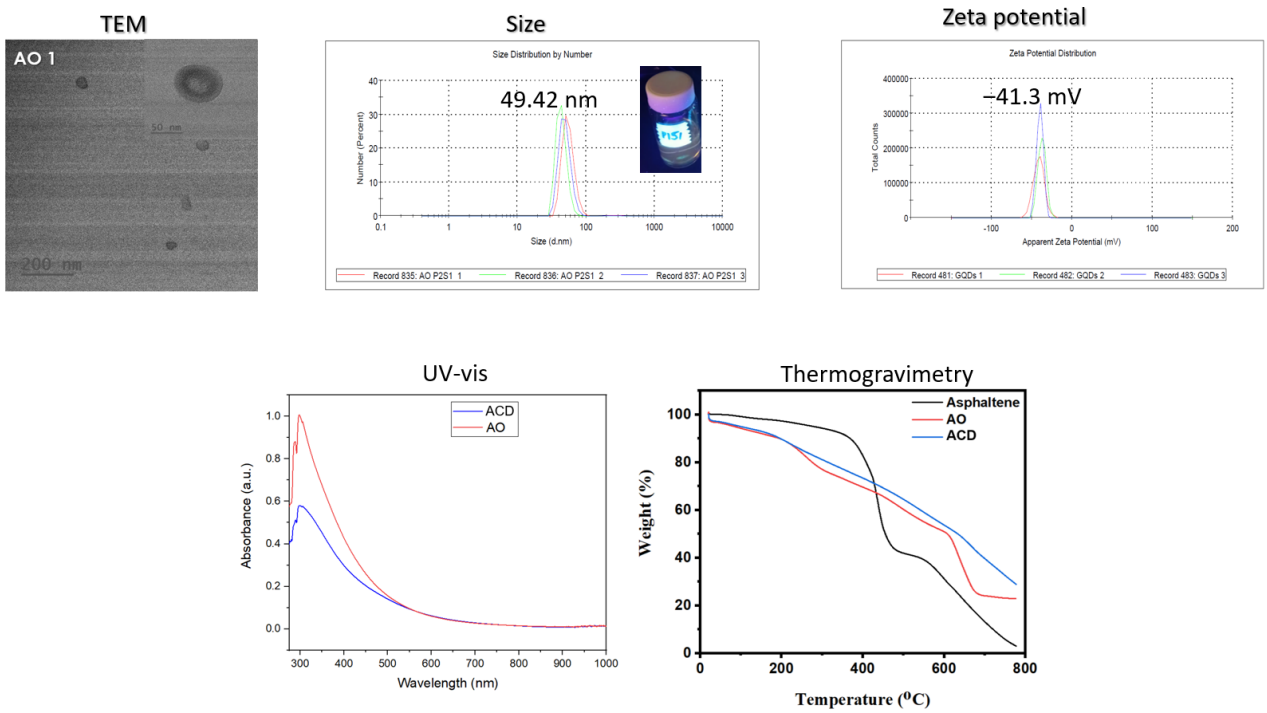

Figure 3: TEM, size, zeta potential, UV-vis, and thermogravimetric analysis of asphaltene oxide (AO). The UV-vis and thermogravimetric analysis of hydrophilic ACDs are also presented for comparison.

The UV-vis spectra of the ACDs and asphaltene oxide show a broad range light absorption between 200 and 900 nm. The wavelength of maximum absorption is about 305 nm in all cases. The thermal stability profiles of the ACDs and asphaltene oxides show similar behavior in general with slight deviation at 600°C for asphaltene oxide synthesized from asphaltenes Sample A. They exhibit near-steady degradation throughout, against the pronounced degradation of asphaltenes at 450°C. The advantageous near-steady degradation profile in the ACDs and asphaltene oxide is attributed to the gradual loss of the functional groups in the nanoparticles. Elemental composition of the hydrophilic ACDs was determined by inductively coupled plasma mass spectrometry (ICP) and compared with that of asphaltenes sample B as presented in Table 1.

Table 1. Elemental analysis of asphaltenes sample B and ACDs from asphaltenes sample B

Elements	Asphaltenes Sample B (mg/kg)	ACDs (mg/kg)
Vanadium	1268.34	58.98
Nickel	649.72	138.93
Sulfur	507.82	872.48
Lithium	6.67	1.46
Iron	157.50	43.27
Sodium	310.87	189.52
Chlorine	490.56	415.94
Potassium	78.19	31.24
Phosphorus	9.98	1.89
Cobalt	3.039	0.64

The data in Table 1 for pristine asphaltenes and the hydrophilic ACDs also show the capability of the acids utilized in this work to substantially reduce the concentrations of trace elements in the asphaltenes precursor, especially vanadium and nickel. We have also established the highly preferential affinity of the hydrophilic ACDs to water by testing their dispersions in various solvents (Figure 4). However, no meaningful dispersion could be obtained in all tested solvents apart from water. It is also interesting to observe that upon the addition of just one drop of water to each solvent-containing vial, the ACDs immediately start responding to some solvents: a testimonial of the superhydrophilicity of the ACDs.

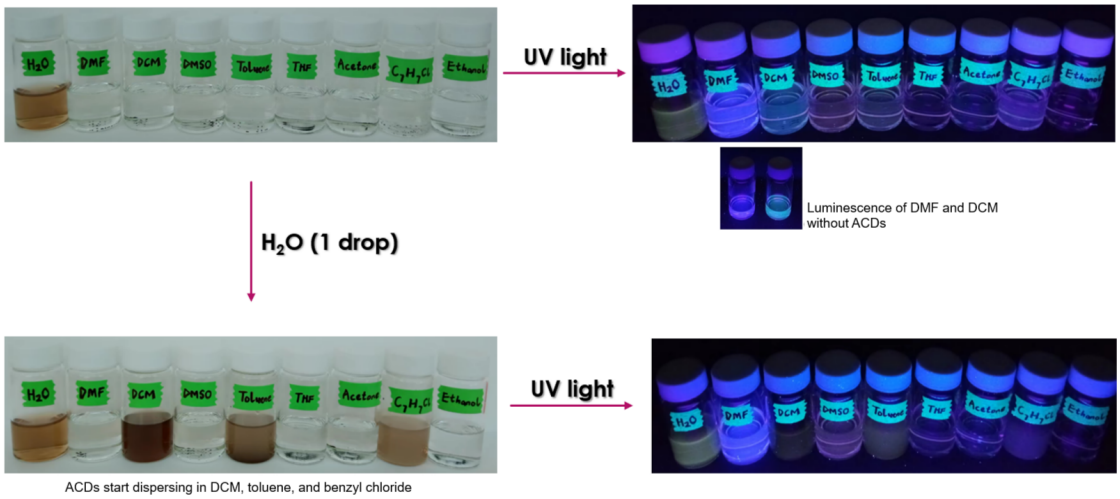

Figure 4. Dispersibility of the hydrophilic ACDs in common solvents.

Detailed rheological study: We have conducted rheological studies ACDs in water before and after 1 hour shear at constant force of 4 N (Figure 5). We observed that the viscosity of the studied dispersions does not depend on the shear rate, which is typical of Newtonian fluids. Also, we exposed these suspensions to a 1 hour of higher shear rates (that cannot be accessed with the rheometer) and probe their rheological signature after. The viscosity of the dispersions remains Newtonian but slightly increases after 1 hour shear. We believe that the super-hydrophilicity of the ACDs because of the numerous oxygen- and nitrogen-containing groups (hydroxyl, carboxyl, ether, and nitro groups) introduced on their surfaces by the acid-based oxidation synthesis causes substantial repulsion of the anions of such groups in solution. This phenomenon highly decreases the tendency of the ACDs to form extended networks even after 1 hour shear. As the major difference between the ACDs and asphaltene oxide is size, the rheological behavior of the asphaltene oxide is not expected to be significantly different. The viscosity profiles of commercial 5 and 20 nm silica nanoparticles are also presented for comparison.

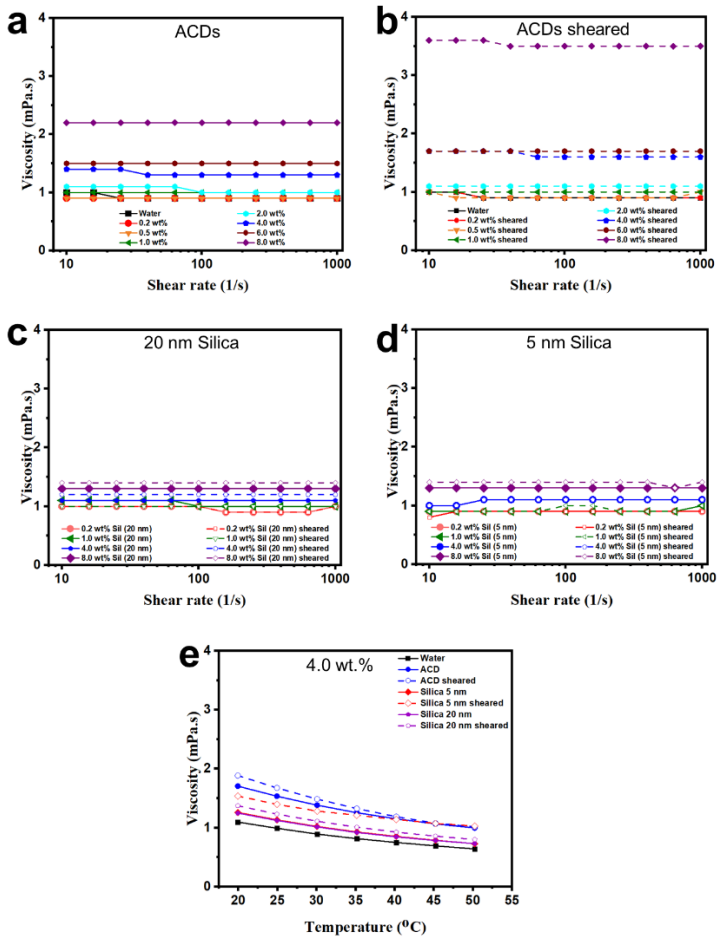

Figure 5: Viscosity of water and the ACDs (a) before and (b) after shearing. Viscosity of (c) 20 nm and (d) 5 nm silica nanofluids before and after shearing. (e) Viscosity of water compared with 4.0 wt.% ACDs and 5 and 20 nm silica nanofluids at different temperatures.

The elemental composition of the asphaltene oxide was determined by inductively coupled plasma mass spectrometry (ICP) and compared with that of asphaltenes sample A as presented in Table 2. The data in Table 2 for pristine asphaltenes and the asphaltene oxide also show the capability of the acids utilized in this work to substantially reduce the concentrations of trace elements in the asphaltenes precursor, especially vanadium and nickel.

Table 2. Elemental analysis of asphaltenes sample A and asphaltene oxide from asphaltenes sample A

Elements	**Asphaltenes Sample A (mg/kg)**	**Asphaltene oxide (mg/kg)**
Vanadium	623.49	9.28
Nickel	1087.65	59.15
Sulfur	1292.65	1385.15
Iron	1163.11	82.83
Sodium	359.92	16.69
Aluminium	578.08	127.108
Phosphorus	59.98	2.36
Cobalt	4.287	0.23
Chromium	31.619	6.38

Metal sensing, water-based lubrication, and thermal conductivity

Investigation of iron sensing: We prepared iron ion stock solution from iron (III) chloride and prepared different working concentrations from the stock solution. The working concentrations were used to spike deionized water, Bow River water, and process (produced water) for iron sensing application. We investigated the ACDs as nanosensors for detection of Fe^{3+} in de-ionized water and real water samples such as Bow River water and produced water (Figure 6). The ACDs showed considerable sensitivity to Fe^{3+} even in the real water samples, which showcases the potential of the ACDs as a nanosensor for practical applications.

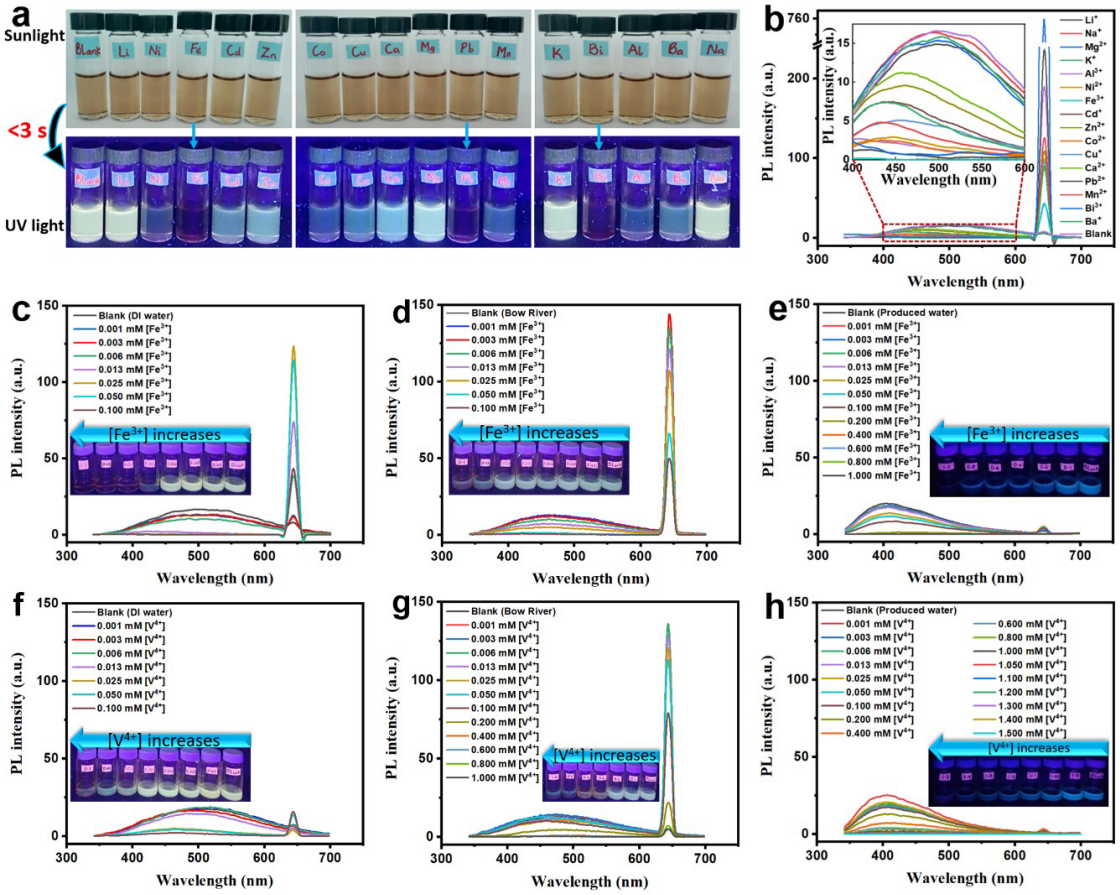

Figure 6. (a) Digital pictures of ACDs dispersion in water before and after adding various metal ions and observed under a UV lamp operated at 365 nm in the dark. (b) Fluorescence spectra of the ACDs dispersion in DI water (pH 7) after adding different metal ions. Fluorescence spectra of the ACDs with various Fe^{3+} concentrations in (c) DI water, (d) Bow River water, and (e) produced water. Fluorescence spectra of the ACDs with various V^{4+} concentrations in (f) DI water, (g) Bow River water, and (h) produced water. Insets show digital images of the ACDs dispersion observed under UV lamp (365 nm) in the dark.

Lubrication studies with nanofluids: We prepared nanofluids with the ACDs via a facile and eco-friendly approach (Figure 7a). This involved dispersing different amounts of the ACDs in water to obtain nanofluids as follows: 0.2, 0.5, 1.0, 2.0, 4.0, 6.0, and 8.0 wt.%. For comparison, two different sizes of commercial silica nanoparticles (5 and 20 nm) were used to prepare nanofluids of different concentrations: 0.2, 1.0, 4.0, and 8.0 wt.%.

We have also investigated the ACDs as water-based lubricant additives, where low concentrations of the ACDs were found to substantially reduce the friction coefficient of water. The hydrophilicity of the nanoparticles is evident from the uniform dispersion of the ACDs and 5 nm silica nanofluids, as seen in their uniform fluorescence in Figure 7b. The friction-reduction performance of water (control), ACDs, and silica (5 and 20 nm) nanofluids at various sliding speeds are shown in the Stribeck curves (Figure 7c-e). At low speeds (boundary regime), the surfaces compress nanoparticles between contacting asperities, and there is no fluid film present. As the speed increases, the entraining fluid increases the normal pressure, causing the surfaces to separate and transition into the mixed lubrication regime. And at higher sliding speeds, the primary friction mechanism becomes hydrodynamic lubrication from a fully formed fluid film.

Interestingly, all ACD loadings substantially reduce the friction factor of water in the boundary regime (surface contact dominated), pointing to their beneficial use as nano-additives for water-based lubricants. Using 4 wt.% of ACD, 8 wt.% of 5 nm silica, and 1 wt.% of 20nm silica, demonstrating the most effective friction-reduction formulation within each nanofluid group, the high boundary friction factor of pure water (~0.65) decreases to 0.26, 0.36, and 0.45, respectively. For the ACDs, the friction factor decreases with loading until 4.0 wt.%, after which it increases for the 6.0 and 8.0 wt.% loadings. A similar increase in friction factor was recorded for hydrophilic graphene quantum dots as water-based lubricant additives above 4.0 wt.%.

Compared to water, both the ACDs and silica nanofluids exhibit a delayed transition to the mixed and hydrodynamic lubrication regimes (Figure 7c-e). The steep drop observed in the mixed regime for water, which indicates a substantial lubricant effect between the steel surfaces, is also reduced with the ACDs and silica (5 and 20 nm) nanofluids. In the hydrodynamic regime, low loadings of 5 nm silica and ACDs (0.2–2.0 wt.%) closely follow the trend of water. Conversely, high loadings (4.0 wt.% and above) do not follow this trend, suggesting that the multiple-body contacts between nanoparticles present in the tribological contact plays a significant role in the lubrication mechanism. In addition to having the highest boundary friction levels, all loadings of 20 nm silica exhibit a similar behavior in the hydrodynamic regime like water. It is interesting to note that above 4 wt.% of the ACDs and with 8 wt.% of 5 nm silica nanoparticles, there is no obvious transition to the mixed and hydrodynamic regimes. The time dependent friction during constant shearing of water, ACDs, and silica nanofluids is presented in Figures 7f-h.

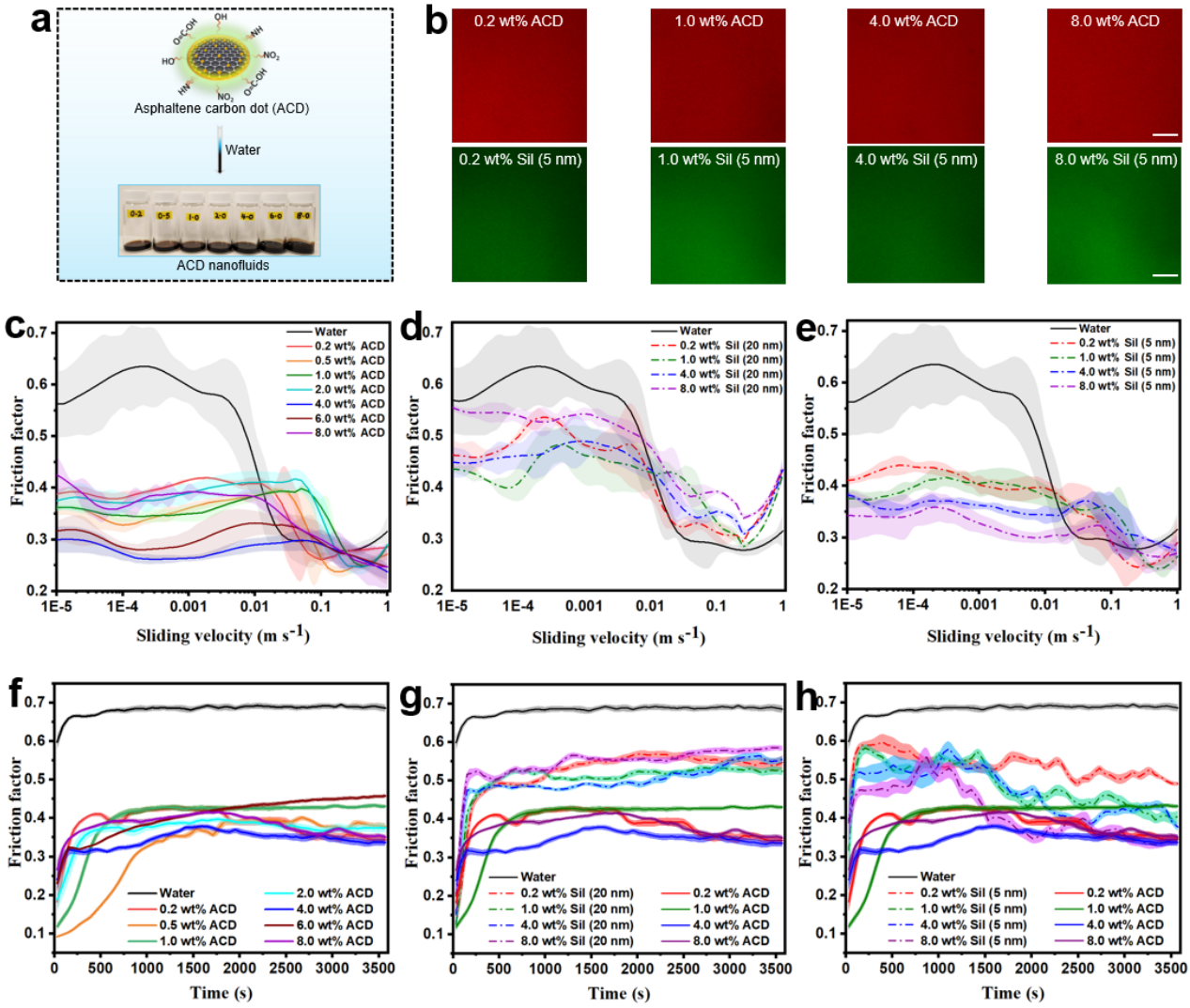

Figure 7: (a) Schematic illustration of the facile preparation of ACDs nanofluids with different ACDs loadings (0.2, 0.5, 1.0, 2.0, 4.0, 6.0, and 8.0 wt.%). (b) LSCM images of representative ACDs and 5 nm silica nanofluids. Scale bars = 20 µm. (c-e) Stribeck curves showing the friction reduction performance of water and different loadings of ACD and silica nanofluids (0.2, 1.0, 4.0, and 8.0 wt.%). (f-h) Time-dependent friction during constant shearing of water, ACDs, and silica nanofluids.

Thermal conductivity evaluation of ACDs dispersions: The ACDs (5 nm) were used to prepare dispersions in water and an antifreeze (car radiator coolant) to study thermal conductivity enhancement in those media. The impressive hydrophilicity of the ACDs is a driving factor for their miscibility in those media. Again, preparation of the dispersions (200, 400, 600, 800, 1000, and 5000 ppm) was also facile and eco-friendly as they were prepared without the need for water bath sonication, probe sonication, etc. Asphaltene oxide samples (95 nm) were also prepared to study the effect of size on thermal conductivity enhancement.

Thermal conductivity of the dispersions was measured, and it was found that the ACDs could improve the thermal conductivity of water, and an antifreeze (car radiator coolant) by 16% and 11%, respectively (Figure 8). The asphaltene oxide samples were also investigated on the different media of water, and an antifreeze (car radiator coolant) and were

found to induce 19% and 20% increase in thermal conductivity, respectively. We concluded that the larger size of the asphaltene oxide (95 nm) is more beneficial to thermal conductivity enhancement than the small size (5 nm) of the ACDs.

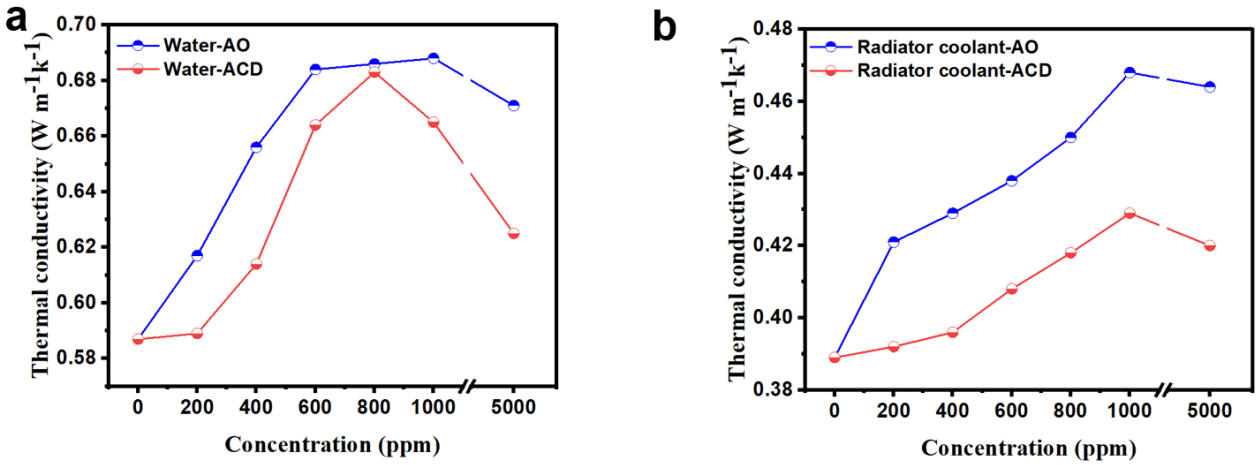

Figure 8. Thermal conductivity of ACD and asphaltene oxide (AO) in (a) water and (b) an antifreeze (car radiator coolant).

Assessing subsurface tracer capability

We prepared metal complexed with ACDs using iron and manganese as metal centers and the ACDs as ligands. This was conducted by complexation chemistry and different concentrations of the metals were used (0.1, 0.2, 0.3, and 0.4 mM). It was found that ACDs could alter proton MRI in contrast with free iron or manganese (Figure 9).

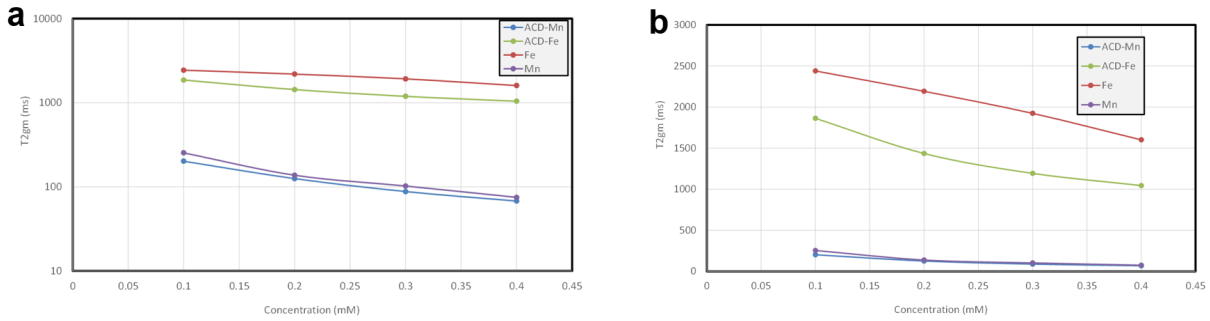

Figure 9. (a) T_2 relaxivity of ACD-Fe and ACD-Mn complexes in water. (b) Their zoomed scale presented for better understanding of the difference that ACDs make.

Additionally, we mounted the micro-sandpack setup in our lab as illustrated in Figure 10. We have also utilized this setup to obtain preliminary results on the retention or not of the ACDs in the micro-sandpack.

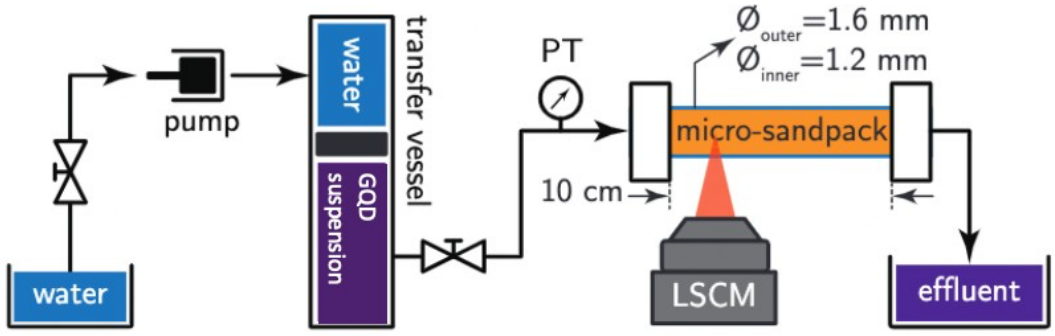

Figure 10: Experimental Micro-Sandpack Setup. A pump delivers water to the bottom part of a transfer vessel that pushed a piston, which in turn made the ACD suspension flow into the lines connected to the porous micro-sandpack. Laser scanning confocal microscopy (LSCM) can be used to image the suspension (model propant) flowing through the micro-sandpack. A pressure transducer (PT) is connected close to the micro-sandpack inlet. The outlet is open to the atmosphere and attached to the effluent fluid collector.

The results with ACD suspension injection into micro-sandpack showed no retention in the porous media, which is promising for the tracing applications. Images collected at various time points of the experiments using laser confocal scanning microscopy and the corresponding effluents reveal the ACDs are super-hydrophilic and traverse the sands with the effluent not losing any fluorescence intensity (Figure 11). As per plan, we will work on the ACD injection with proppant in the upcoming year.

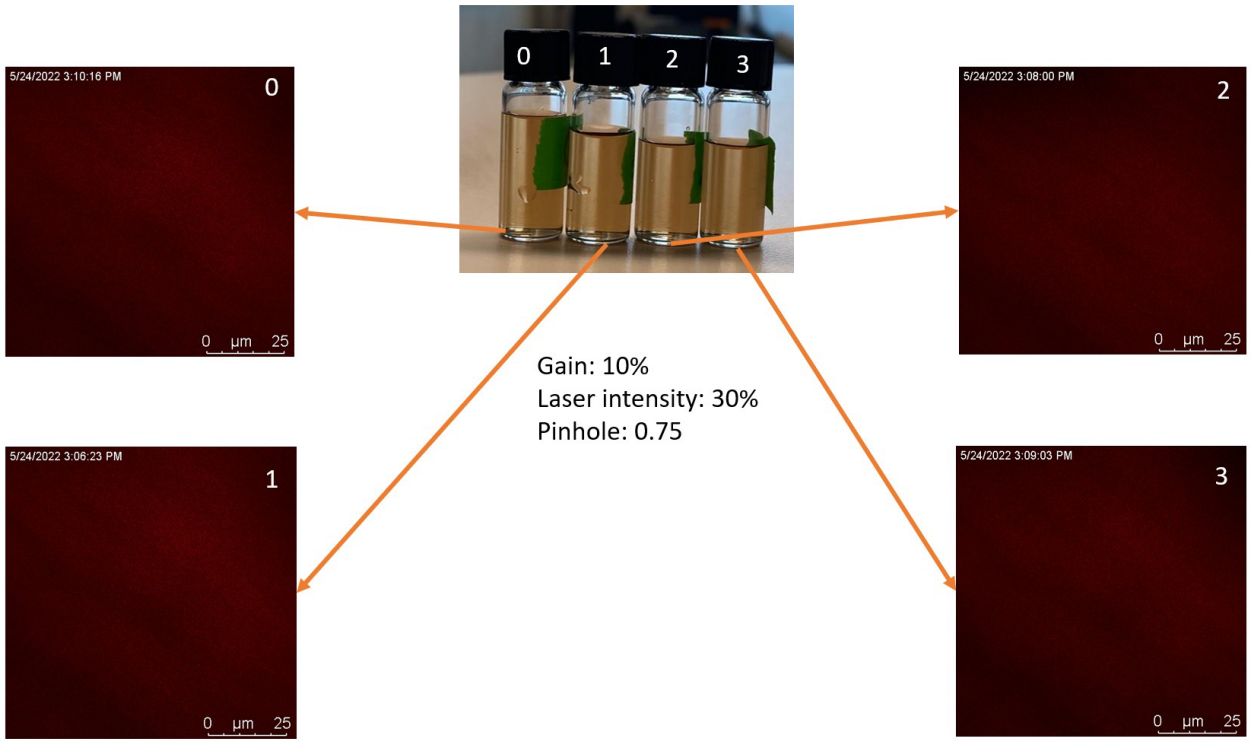

Figure 11: Time-course images of the hydrophilic ACDs during flushing in core flood micro-sand pack.

Considering these promising results, the ACD-Fe complex was further explored on a 9.4T MRI equipment. It could be seen that the ACD-Fe complex could decrease proton MRI signal in T_2-weighted imaging (Figure 12).

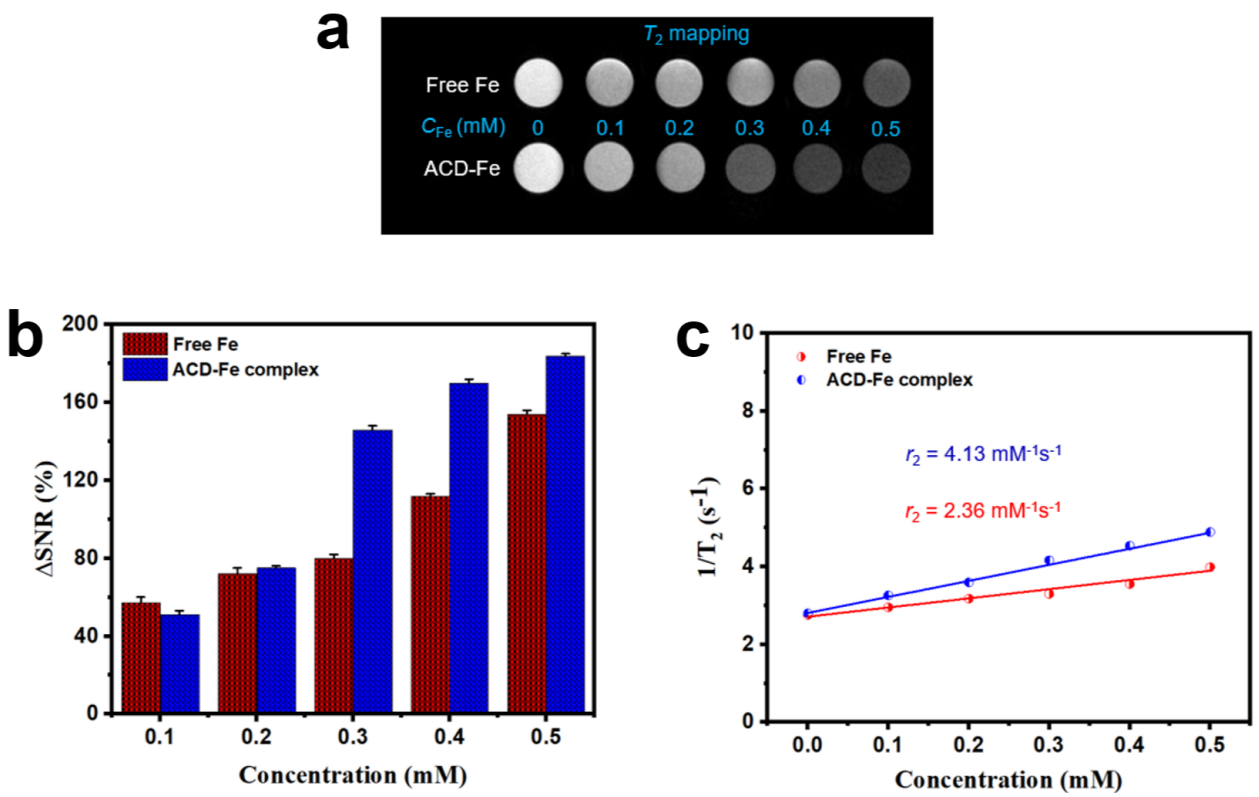

Figure 12. (a) T_2-weighted in vitro MRI of free Fe^{3+} and ACD-Fe complex in water on a 9.4 T scanner. (b) Quantitative analysis of the signal enhancements obtained with free Fe^{3+} and ACD-Fe complex as measured with the ImageJ software. (c) Plots of transverse relaxation rates of free Fe^{3+} and ACD-Fe complex as functions of Fe^{3+} concentrations.

Tumor imaging and therapeutic probe

Bio-based characterization of GQDs:

Cancer is one of the diseases ravaging our society today and ranked top in the leading causes of deaths worldwide. Early diagnosis and treatment have been pinpointed as crucial strategies to reduce mortality rates. Even though various established cancer treatment modalities exist today, new treatment modalities continue to evolve. One of such new modalities is near infrared (NIR)-mediated photothermal therapy, takes advantage of the transparency of biological tissues in the NIR region, enabling photothermal agents to effectively convert optical energy to heat energy with minimal invasiveness. NIR cancer photothermal therapy requires the use of certain photothermal agents (e.g., gold nanoparticles, CuS nanoparticles, conductive polymer nanoparticles, and indocyanine green dye) that absorb light and convert same to heat

to ablate cancer cells locally. Unfortunately, the inorganic-based agents exhibit long-term toxicity and low photostability from the well-known 'melting effect' peculiar with metals. Polymeric nanoparticles and organic dyes on the other hand exhibit low photoconversion efficiency and photobleaching, respectively. Until now, there has been no report on the (i) photothermal properties of any asphaltenes-based material, and (ii) utilization of any asphaltenes-based material for cancer imaging and/or therapy.

Asphaltenes present a low-cost precursor for high-value materials engineering. An epitome of this is the asphaltenes-derived carbon dots (ACDs) developed in our laboratories which have shown intrinsic fluorescence properties and impressive water dispersibility; a highly sought after parameter for biomedical materials especially for cancer treatment and diagnosis.

It is common knowledge that cytotoxicity is crucial in cancer imaging and therapy. We have established that the ACDs are considerably benign according to in vitro biocompatibility tests we conducted with 4T1 murine cancer cells (Figure 13a). This was confirmed in vivo as mice injected with up to 150 and 200 µL of 1.5 mg/mL ACDs could survive up to 24 h post-injection (Figure 13b). Moreover, the intrinsic fluorescence properties of the ACDs could be leveraged to simultaneously provide fluorescence imaging of cancer cells alongside photothermal therapy in line with the popular imaging-guided cancer therapy mantra (cancer theranostics).

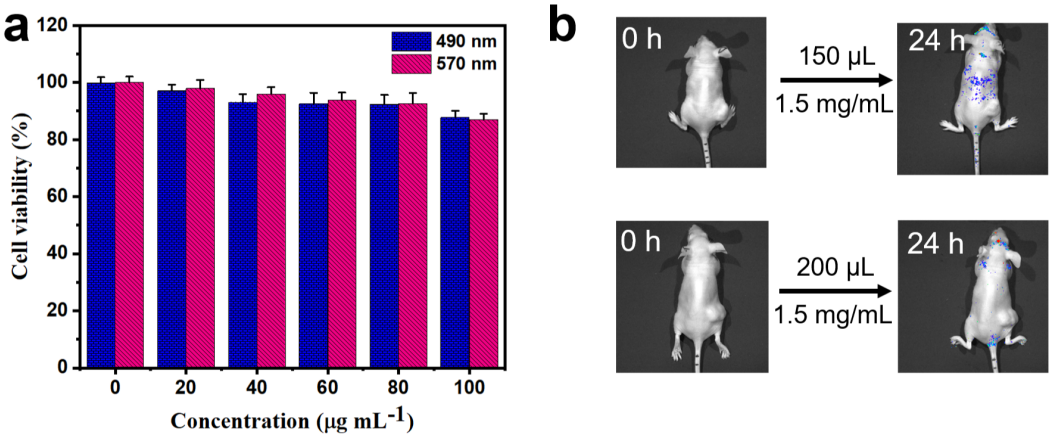

Figure 13. (a) In vitro cell viability of 4T1 cells co-incubated with the ACDs for 24 h. (b) In vivo cytotoxicity evaluation of nude mice before and 24 h post-injection with 150 and 200 µL of 1.5 mg/mL ACDs.

Water dispersibility is a huge challenge for nanomaterials designated for biomedical application. It is noteworthy that our ACDs possess impressive hydrophilicity as high as 275 mg/mL that outperforms those of most commercial nanomaterials. The dispersion of 275 mg/mL of the ACDs in water was established by observing the dispersion in a laser confocal microscopy and the obtained 3-D image is shown in Figure 14a. The appreciable fluorescence property of our ACDs has been established which we expect to deploy for tumor imaging

(Figure 14b). Our preliminary tests also reveal that the ACDs are not photobleached upon extensive irradiation unlike most commercial organic dyes for tumor imaging. This was established when a given dispersion of the ACDs was exposed to excitation at different wavelengths cumulatively amounting to about 70 min of constant irradiation (Figure 14c).

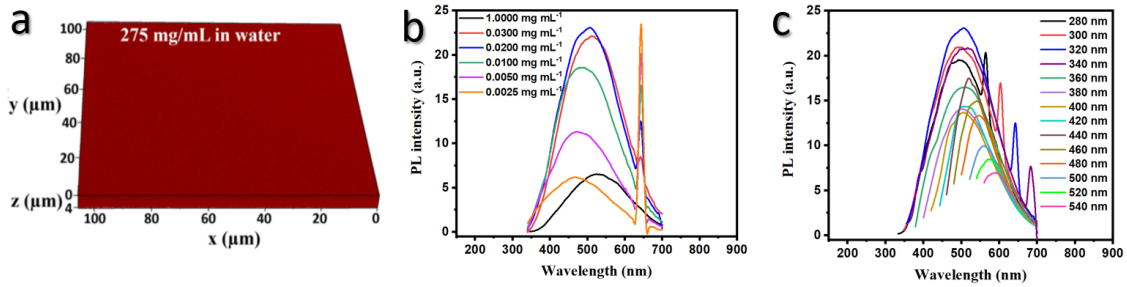

Figure 14: (a) 3D confocal microscopic image of 275 mg mL-1 ACDs dispersion in water. Fluorescence spectra at different (b) concentrations of the ACDs and (c) excitation wavelengths using 0.02 mg/mL ACDs in water.

We have also established appreciable compatibility of the ACDs in typical physiological environment using phosphate buffer saline (PBS) and could detect two important human antioxidants ascorbic acid (AA) and glutathione (GSH) in such an environment (Figure 15a-b). Moreover, the ACDs still exhibit appreciable luminescence in complex biological systems such as human urine and could considerably detect the antioxidants therein (Figure 15c-d).

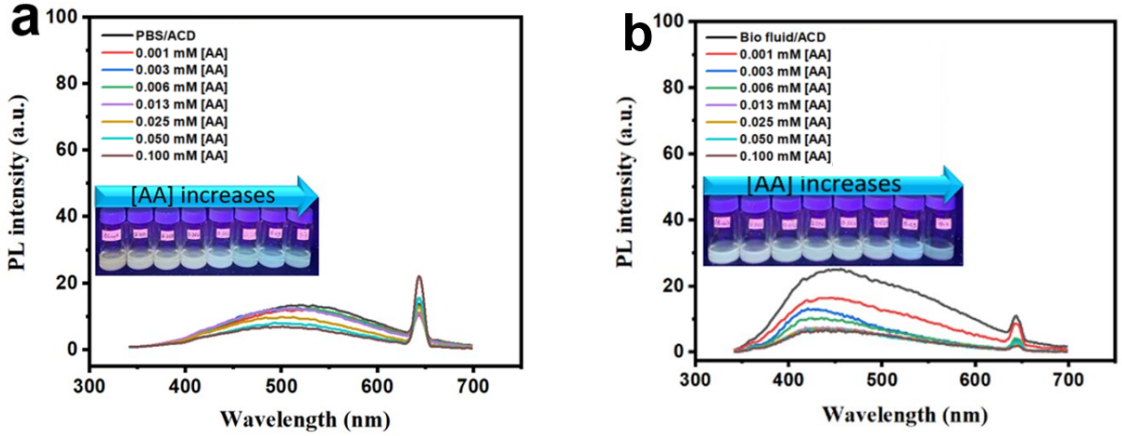

Figure 15: Fluorescence spectra of the ACDs dispersion with various concentrations of AA in (a) PBS and (b) biological fluid (human urine).

In-vitro tumor photothermal imaging and therapeutic studies: Interestingly, we have established significant heat generation from water dispersions of our ACDs upon NIR laser

irradiation. It is interesting to note that 100 µg/mL ACDs provides about 20°C temperature elevation in 5 min upon laser irradiation at 1 W/cm^2, which is only comparable to that of gold nanoparticles as it outperforms those of the popularly researched conducting polymer (polypyrrole) and the FDA-approved indocyanine green dye for clinical use. Temperature rises from different concentrations of our ACDs upon 1.0 W/cm^2 laser irradiation shows the ACDs could generate the minimum amount of heat (42°C) required to locally ablate cancer cells in typical photothermal therapy (Figure 16a).

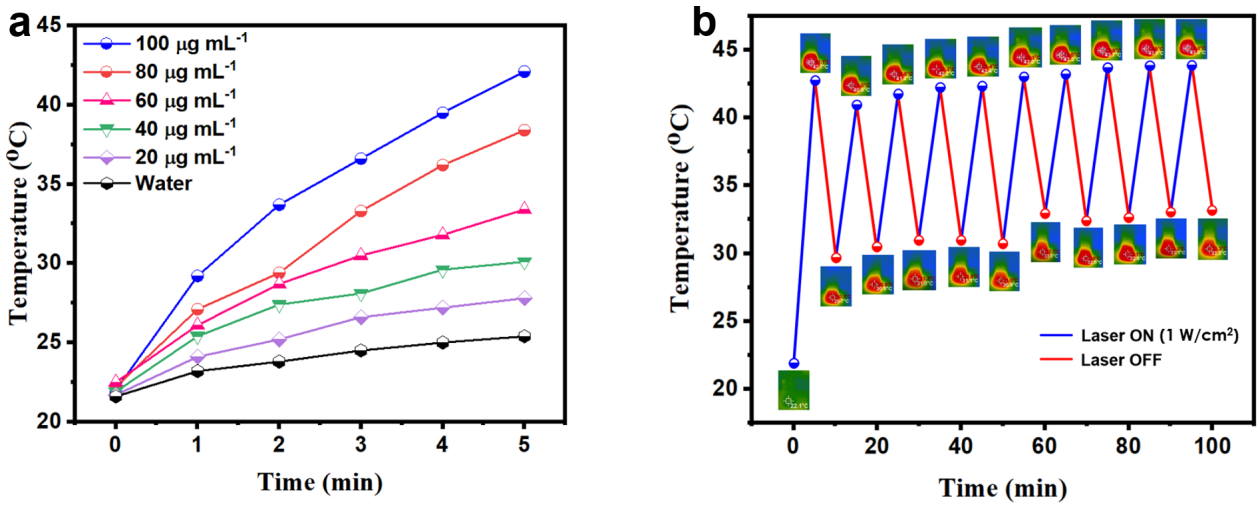

Figure 16. (a) Temperature variations of different concentrations of ACDs upon an 808 nm laser irradiation at 1.0 W/cm^2 for 5 min. (b) Temperature variations of 100 µg/mL ACDs upon an 808 nm laser irradiation at different power densities for 5 min.

Notably, the ACDs offer photothermal stability for more than ten laser on/off cycles which is not attainable with the clinically approved indocyanine dye (Figure 16b). This confirms that that ACDs could be used to achieve long-term fluorescence imaging and prolonged heat generation in target cancer cells to elicit cell death and consequent cancer treatment.

In-vivo photothermal imaging and phototherapy in tumor-bearing mice

This task has been completed too. Animal models (mice) for the *in vivo* experiments were acquired and inoculated with 4T1 tumor cells. The animals were later injected with ACDs and exposed to near infrared irradiation. Another group of the animals were injected with phosphate buffer saline (PBS) to serve as control. Photothermal images of the tumor region were acquired at different time points leveraging the light-to-heat conversion capability of the ACDs (Figure 17a). At 15 days post-irradiation, the tumors in the animals were excised and measured to visualize the photothermal treatment outcome (Figure 17b). Upon hematoxylin and eosin staining, tumor of mice treated with the ACDs showed significant cell death (Figure 17c), confirming the

capability of the ACDs to convert near infrared light to heat and elicit tumor cell death in typical photothermal therapeutic modality.

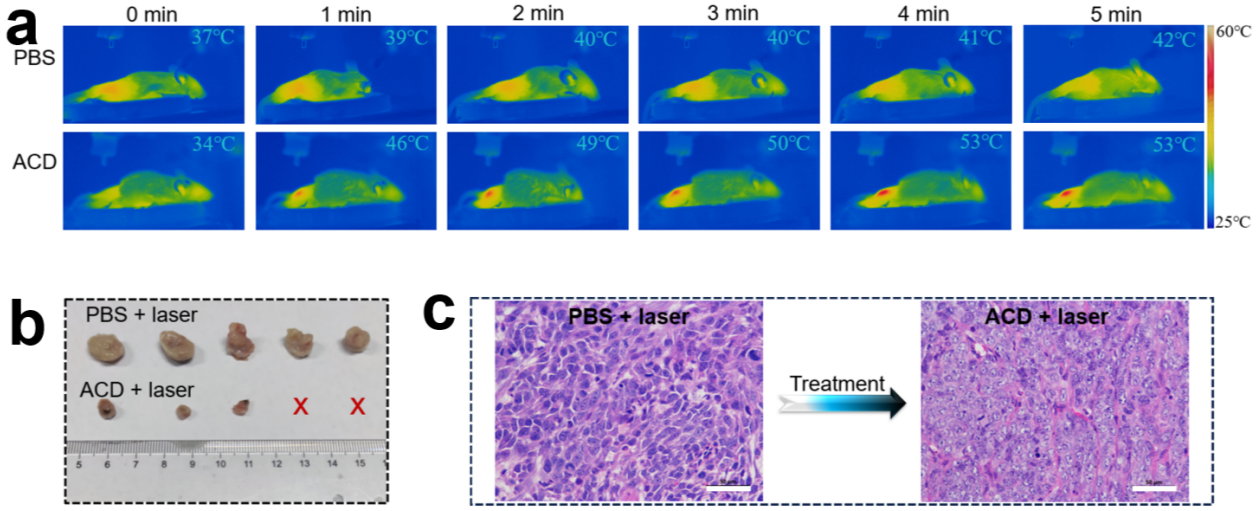

Figure 17. (a) Time-course NIR photothermal images of whole mice revealing the tumor region upon laser irradiation (800 nm; 1.5 W cm-2) of the ACDs. PBS served as control. (b) Representative digital images of the tumors excised from mice treated with ACDs and PBS at 15 days post-treatment. (c) Hematoxylin and eosin staining micrographs of tumors excised at 15 days post-treatment with ACDs and PBS (control). Scale bar = 50 µm.

Other applications of the ACDs we have explored

High interphase Pickering emulsion stabilization:

We have used the ACDs to stabilize high interface Pickering emulsions (HIPEs). High Internal Phase Emulsions (HIPEs) represent a particular class of emulsions in which the internal phase occupies more than 74% of the total volume. HIPEs can be classified into surfactant-stabilized HIPEs and particle (colloid)-stabilized HIPEs. Surfactant-stabilized HIPEs employ low molecular weight surfactants like sodium dodecyl sulfate, to higher molecular weight polymeric surfactants, as their stabilizing agents. These surfactants, encompassing both ionic and nonionic variants, are highly effective in reducing interfacial tension, which lends to the emulsion's stability. In contrast, particle stabilized HIPEs, also known as Pickering emulsions, use solid particles as stabilizers instead of surfactants. Various solid particles, including polysaccharides, synthetic polymers, and inorganic materials like silica have been employed to stabilize HIPEs. HIPEs find utility in an array of applications such as precursors to produce polymeric foams, controlled-release drug delivery systems owing to their distinct structure and properties. HIPE has also been utilized in the 3D printing of structures including different shaped products, such as numerals, letters, and an array of shapes.

We prepared the ACDs-stabilized HIPEs by adding the oil phase to the ACDs suspension in water. The ACDs used for this study were prepared by two different synthesis methods and designated as ACD1 and ACD2. After a homogenization process of 2 min, phase separation occurred in the emulsion containing ACD2, proving the suitability of ACD1 in stabilizing the emulsion (Figure 18a).

Using contact angle measurements, values of 29.33° for ACD2 and 61.12° for ACD1 were obtained. The calculated detachment energies for ACD1 and ACD2 were 90.45 and 5.56 J/kT, respectively. This implies that ACD1 possesses more than 16 times the detachment energy of ACD2 as shown in Figure 18b. The closely packed double layer maximum capillary pressure was calculated as 78.36 and 112.7 MPa for ACD1 and ACD2, respectively (Figure 18c). Notably, the maximum capillary pressure for ACD2 is approximately 1.4 times greater than that for ACD1. We found that ACD1 possesses a tenfold greater probability of stabilizing oil-in-water emulsions compared to ACD2. Figure 18d shows the relationship between complex probabilities and contact angles with specific data points for ACD1 and ACD2 highlighted as stars.

To further elucidate the influence of particle size on the emulsion stabilization mechanism, particle adsorption at the oil–water interface and the stability of thin film between droplets were studied. A notable observation is that with an increased radius, the detachment energy surges, exhibiting a 204-fold increment (Figure 18e). Such a significant rise in detachment energy underscores its dominance, ensuring that particles are irreversibly adsorbed to the interface, especially when the detachment energy greatly surpasses the thermal energy in several orders of magnitude, as corroborated by existing literature. Concurrently, the results reveal approximately 15 times decrease in the maximum capillary pressure for a radius of 50 nm. Considering the several order of magnitude of elevated detachment energy and the pronounced decrease in maximum capillary pressure, particles are likely to form multiple adsorbed layers at the interface. Such behavior suggests a preference for the particles to migrate to the oil–water interface rather than remaining within the thin liquid film. This predisposition could potentially lead to the thinning out of films, subsequently facilitating the formation of droplet bridges, to stabilize the emulsion. However, given the diminished maximum capillary pressure, it is evident that capillary forces would not act as the primary stabilization mechanism for the emulsion in the scenarios where radius is increased to 50 nm.

The LSCM image in Figure 18f depicts the emulsion stabilized by ACD1. ACD1 and dodecane (oil phase) are the red and black signals, respectively. ACD1 appears uniformly distributed in the water phase with no evident aggregation. However, the intrinsic fluorescence of ACD1 limits our ability to discern variations in particle concentration in the thin aqueous film and at the oil–water interface, particularly at high particle concentrations. Consequently, a particle loading of 0.0025 wt% with a 0.5 oil volume fraction was used to enhance visibility (Figure 18g). This unique representation is noteworthy, as there are yet to reports in literature on successful

emulsion stabilization with such low loading for 50:50 oil-in-water emulsion. Figure 18g shows the bulk of ACD1 are dispersed within the aqueous medium, forming a uniformly spread and robust ACD1 network and few particles wide order layer of particle adsorbed at the oil–water interface which corroborate our theoretical calculations. The ACD1 possesses energy approximately 100 times greater than thermal energy (kT). This suggests that they can be adsorbed at the oil–water interface to form few particles wide layers around the oil. However, the detachment energy is not several orders of magnitude higher, which would lead to irreversible adsorption, forcing all particles to migrate to the interface. Therefore, ACD1 maintains a dynamic equilibrium between the interface and the continuous phase. Owing to their small size of 7 nm, ACD1 have a very high surface area and can cover the entire oil–water interface with a minimal particle loading. They exert such strong capillary forces that they can resist the thinning of the liquid film between interfaces. This resistance helps counteract external pressures, gravitational effects, and potential vibrations during usage and transportation. Furthermore, ACD1 network in water also owes its strength to the high surface charge of ACD1, which results in high colloidal stability and a reduced likelihood of particle aggregation which could minimize the capillary pressure due to increase in the size of particles upon aggregation.

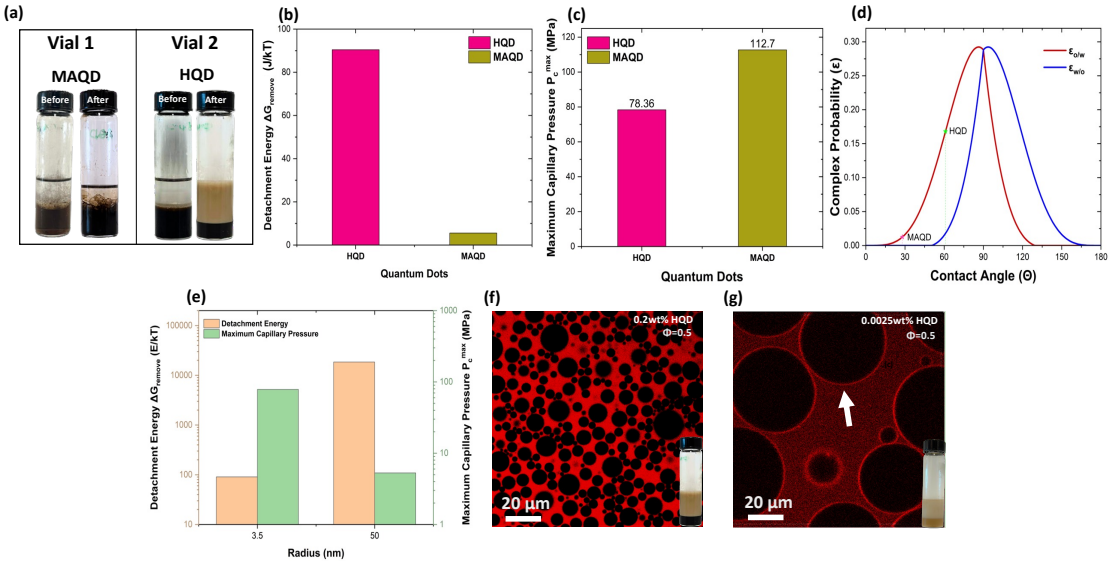

Figure 18. Digital images of vials both pre- and post-homogenization containing ACD1 and ACD2 in the water with oil phase. (b) Detachment energy, (c) maximum capillary pressure, and (d) complex probability for stabilizing of oil in water emulsion and water in oil emulsions for both ACD1 and ACD2. (e) Effect of change in radius on the detachment energy and maximum capillary pressure of the ACD1. LSCM images of (f) 0.2wt% and (g) 0.0025wt% ACD1 stabilized emulsions with 0.5 oil volume fraction. The red and black signals represent the ACD1 and dodecane (oil phase), respectively. White arrow depicts the ACD1 adsorption at the oil–water

interface.

The extrusion-based 3D printing was utilized for the printing of 3D constructs from ACD1-stabilized HIPEs (Figure 19a). The successful deployment of this printing strategy to produce letters exhibiting round forms, straight lines, and significant curvatures is demonstrated in Figures 19b-c. The layering process upon printing is distinctly evident in the lateral perspective of the square, as shown in Figure 19c. This denotes the potential of HIPE to fabricate entities of geometric intricacy on a millimeter-scale. Remarkably, our ACD1-stabilized HIPEs exhibited an extraordinarily low total particle loading of 0.075wt%, operating in neutral pH. Moreover, the infill density and printing parameters can be customized in accordance with the specific requirements for 3D print fabrication. The introduced strategy offers an innovative formulation method for HIPEs based 3D printing that demonstrates high tunability and flowable behavior without the requirement for high stabilizer concentrations.

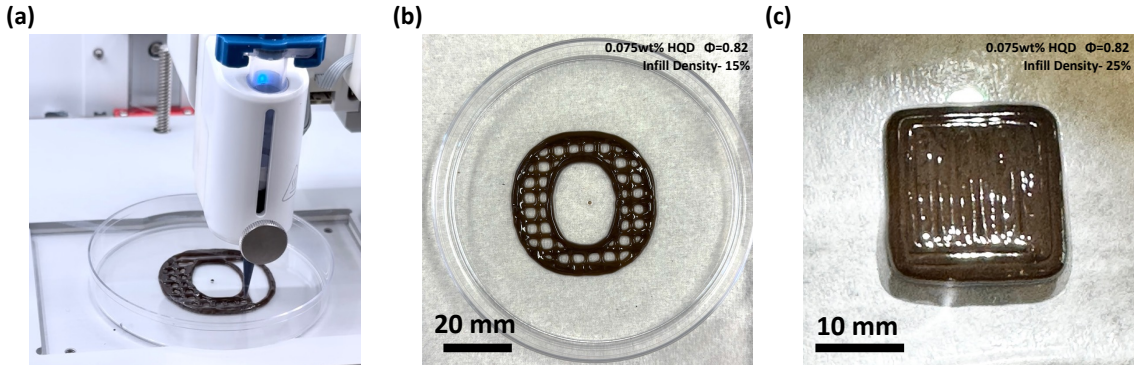

Figure 19. (a) Set up of 3D structure printing by extrusion using ACD1-stabilized HIPEs. (b) Overhead perspective of the shape "O". (c) Top view of a square, illustrating the various stratifications of the emulsion ink. These images were captured at 1 h post-printing under ambient conditions.

Holographic sensing with ACDs/polymer composite

We utilized the ACDs as a component of holographic sensor material. Holography is an important application field. The image produced by a hologram has the advantage of a 3D effect and realistic depth perception. Photopolymer-based holography has emerged as a valuable technology in photonics, finding diverse applications such as holographic sensors, holographic data storage, 3D displays, self-written waveguides, photolithography, and neutron optics. Recent advances in the design of lasers and novel adaptable holographic recording materials have contributed to the rapid growth of new holography applications, which are expected to significantly impact our daily lives. Photopolymer films are an attractive

option for holographic sensors which rely on dimensional and average refractive index-based changes in the volume grating, as they are flexible and can be selectively functionalised for analytes using nanoparticles and other chemical agents. Several investigators have demonstrated that the addition of solid inorganic nanoparticles to different photopolymer materials improves holographic properties of the resulting nanocomposite. A main drawback of these materials, however, is their significant scattering.

The size and concentration of nanoparticles in a photopolymer material allow for alteration of the properties of the light interacting with them. Specific concentrations of nanoparticles can capture the phase and polarization of light and re-emit it with high levels of accuracy. Nanocomposite materials are dependent on the volume percentage of the nanomaterial that is incorporated into the bulk material, and the refractive index of that nanomaterial. The incorporation of ACDs should allow for the increase in this refractive index while allowing the polymer to retain its transparency.

Figure 20a. presents the variation in refractive index with respect to wavelength for undoped and at different concentrations of the ACDs nanocomposite films. PVA with refractive index of 1.477 was used as a bulk for the distribution of the ACDs. The refractive index of the nanocomposite samples was measured using a refractometer at two different wavelengths, 532 and 632 nm, with peak refractive indexes of 1.552 ± 0.019 and 1.549 ± 0.027 measured respectively. The increase in refractive index of the photopolymer/ACDs nanocomposites in comparison with pure undoped photopolymer are in line with the predictions of the Bhar and Pinto model. However, the decrease in refractive index of the nanocomposite films observed at 1.5 and 2.0 wt% concentration may be due to the phase separation and agglomeration of nanoparticles within the polymer matrix. Other properties of the holographic sensing composite such as Refractive index modulation, Diffraction efficiency, and Bragg selectivity are presented in Figure 20b-f.

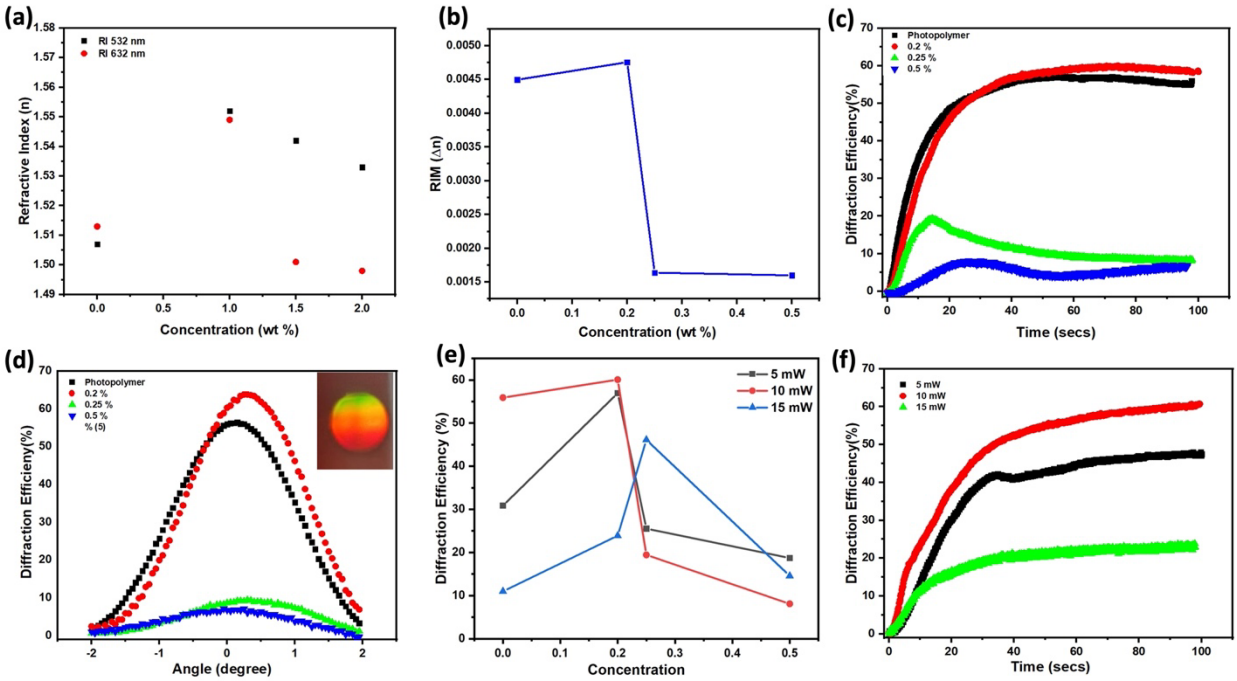

Figure 20. (a) The variation in refractive index (n) with respect to wavelength (λ) for undoped and at different concentrations of HQDs nanocomposite films (b) Refractive index modulation (RIM) in 30 µm-thick layers. (c) Diffraction efficiency (DE) versus the exposure (recording) time at 0.2 %, 0.25 % and 5 % concentrations. (d) Bragg selectivity curve of the transmission grating at 0.2 %, 0.25 % and 5 % concentrations recorded using 5 mW/cm^2. (e) Diffraction efficiency versus exposure energy at different concentrations (f) Diffraction efficiency versus the exposure (recording) time with a recording intensity of 5, 10 and 15 mW/cm^2.

In vivo tumor MRI

We also used the ACD-Fe complex as a contrast agent for tumor MRI in vivo. MRI images of whole mice body were taken at various time points post injection of the ACD-Fe complex (Figure 21). It was observed that the ACD-Fe complex could increase the MRI signal in the tumor region after 1 h injection. Appreciable signal enhancement could also be observed up to 4 h post-injection, suggesting the possibility of using the ACDs as a cheap MRI contrast agent in biomedicine for prolonged tumor imaging.

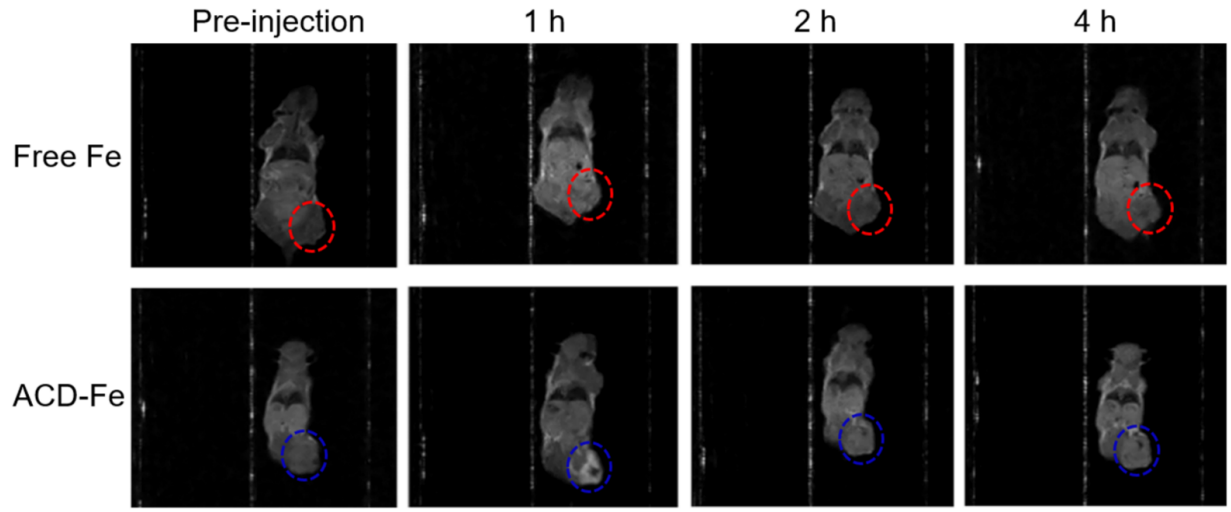

Figure 21. Time-course T_1-weighted in vivo magnetic resonance images of 4T1 tumor-bearing nude mice injected with free Fe^{3+} and ACD-Fe complex. The red and blue doted circles represent the tumors.

Project Succes Metrics

In our lab already, we could utilize 20 g of asphaltenes in one synthesis run to obtain substantial yield (>57%) of the ACDs whose sizes are below 20 nm. This shows we can meet a 10 kg/day production of the ACDs in the commercialized scale. Our facile synthesis route enabled us to tune the fluorescence of the ACDs to achieve five different wavelengths between orange and blue. In terms of hydraulic fracking tracing, we prepared metal complexed ACDs, tested their capability for MRI to enable hydraulic fracking tracing by the MRI modality, and we demonstrated less than 5% retention of the ACDs in core flood apparatus at the lab scale. As regards the biomedical aspect, we have already established selective uptake of the ACDs by tumor cells, where the ACDs accumulate mainly in the cell nucleus and could map the cell membrane. We also established tumor photothermal imaging, tumor photothermal therapy, and tumor MRI imaging with the ACDs for prolonged time (4 h). We have also established considerable biocompatibility and excellent water re-dispersibility of the ACDs which position them as promising candidates for broader biomedical application. Intermediate product quality in terms of the structure and composition of the asphaltene oxide intermediate has already been determined and they have been utilized in various applications such as antifreeze additives for thermal conductivity enhancement in car radiator coolants.

F. KEY LEARNINGS

Please provide a narrative that discusses the key learnings from the project.

- Describe the project learnings and importance of those learnings within the project scope. Use milestones as headings, if appropriate.
- Discuss the broader impacts of the learnings to the industry and beyond; this may include changes to regulations, policies, and approval and permitting processes

RESPOND BELOW

The successful synthesis of ACDs from various sources of asphaltenes enabled us to learn how to optimize our design strategy to adapt it to various asphaltenes sources. We have optimized the temperature, oxidizing agents and their combination ratio, and synthesis time that ensures adequate recovery of the ACDs during short synthesis times. The key innovation in our approach comes from the solvent pretreatment of the asphaltenes to ensure that they are highly susceptible to acid-mediated oxidization for converting them to ACDs. We are now sure of the best time to isolate asphaltene oxide during the synthesis of ACDs from asphaltenes. And we have also proved that the approach is robust with respect to the variation in the asphaltene source. The composition determinations enabled us to properly understand the structure of the synthesized ACDs to guide their deployment in the target applications and equip us with adequate information to unravel other applications they can be suited. The same goes for the asphaltene oxide, where our learning of their structure and composition has informed us to explore their thermal conductivity to deploy them as antifreeze additives for thermal conductivity enhancement. We have also learnt that ACDs are highly re-dispersible in water which is an outstanding parameter for nanomaterials intended for in vivo applications. We have also learned that ACDs are biocompatible and could effectively convert near infrared light to heat which was leveraged to cause rise in local temperature in tumor cells to elicit cell death and consequent tumor therapy. We learned that the excellent re-dispersibility of ACDs could help in evading particles aggregation when they are applied as water-based friction lubricants, where their abundant oxygen and nitrogen-containing groups provide numerous sites for attachment to steel surfaces to protect wear on steel. Part of the learning from the milestones also includes the successful utilization of ACDs to stabilize high interface Pickering emulsions at high oil volume fractions without the need for additional surfactants. The ACDs-stabilized high interface Pickering emulsions thus possesses flowable properties that enable using the emulsions in 3D printing of different shapes. We also learned that the ACDs could disperse well with various polymers, exemplified by our incorporation of the ACDs into polyvinyl alcohol to generate a holographic sensing material, where the ACDs could enhance the refractive index modulation. Based on the variety of surface functionality of ACDs, we learned that it is possible to use them as ligands to complex metal ions to form ACD-metal complexes that serve as contrast agents for tumor imaging by MRI.

G. OUTCOMES AND IMPACTS

Please provide a narrative outlining the project's outcomes. Please use sub-headings as appropriate.

- **Project Outcomes and Impacts:** Describe how the outcomes of the project have impacted the technology or knowledge gap identified.
- **Clean Energy Metrics:** Describe how the project outcomes impact the Clean Energy Metrics as described in the *Work Plan, Budget and Metrics* workbook. Discuss any changes or updates to these metrics and the driving forces behind the change. Include any mitigation strategies that might be needed if the changes result in negative impacts.
- **Program Specific Metrics:** Describe how the project outcomes impact the Program Metrics as described in the *Work Plan, Budget and Metrics* workbook. Discuss any changes or updates to these metrics and the driving forces behind the change. Include any mitigation strategies that might be needed if the changes result in negative impacts.
- **Project Outputs:** List of all obtained patents, published books, journal articles, conference presentations, student theses, etc., based on work conducted during the project. As appropriate, include attachments.

RESPOND BELOW

Clean Resources Metrics

Metric	Project Target
Investment in 4 Core Strategic Technology Areas	Yes
TRL advancement	3 to 5
Future Capital Investment	$3,000,000
Students Trained (M.Sc., Ph.D., Postdoc)	6
Publications	2 to 4
New Spin-Off Companies created	0
Patents & Records of Invention filed	1

Clean Resources Metrics:

Our team has innovated and secured a patent for a novel and scalable method of creating valuable products, ACDs, with properties independent of the asphaltene origin. This advancement has notably resolved a significant challenge in generating carbon dots with consistent properties from diverse asphaltene sources. Furthermore, these materials have exhibited exceptional performance across a variety of applications (as outlined above).

This project achieved the demand of clean resources from investment in 4 core strategic areas, specifically clean energy and health innovation. We also advanced the tech in the energy and biomed field to the TRL 5 (simulated environment). The commercialization process of this project which is underway is geared towards attracting future capital investment up to $3,000,000 in the coming years. One MSc student, one undergraduate intern, and three postdocs were trained during this project. In terms of publications, one article on friction reduction with the ACDs titled “Unravelling water-based lubrication with carbon dots of asphaltenes origin” has already been accepted for publication last week in the prestigious ACS Applied Materials & Interfaces journal. Two other research manuscripts on tumor MRI, tumor photothermal therapy and photothermal imaging are submitted, three more articles on holographic sensing and HIPE emulsions and thermal conductivity enhancement are in the final stages of preparation. A review article on high-value materials generation from asphaltenes is also ready for submission. Therefore, we expect to exceed our target when it comes to publications and publish 6 articles out of this project. A provisional patent has already been filed on this technology in 2023 as per orginal plan .

Program Specific Metrics:

Program Specific Metrics

GHG emissions: Actual reductions from project	Project Target
# of End Users participating	1 to 3
Unique product/process	1

We have engaged with two end users who are now testing the developed ACDs for lubrication applications. We are actively seeking to engage more end users and discover new markets for ACDs. We believe we have now two unique products (ACDs and AOs) developed from this project.

Project outputs:

With consideration of intellectual property protection, some aspects of the project have been presented in conference such as:

(1) Calgary Innovation Fair,

(2) Alberta Quantum Summit,

(3) Canadian Chemical Engineering Conference, and

(4) Alberta Biomedical Engineering Conference.

Whereas the first three presentations were oral, the last was a poster presentation. In all cases, there was no requirement of either submission or publication of abstracts. Industrialists and researchers discussed with us various aspects of the project, with particular emphasis on the biomedical aspect. We noticed that they have great enthusiasm to eventually see an asphaltene-derived material landing in the biomed world. Another interesting aspect of the discussions was the hydrophilicity of the ACDs, which is above par.

As regards the publications from this project, one manuscript has already been submitted for publication based on the water-based friction reduction studies. Two other manuscripts on tumor MRI and tumor photothermal imaging/therapy with the ACDs are ready for submission.

Meanwhile, this project has garnered the interest of industrialists as two letters of support have been successfully obtained from two companies who are impressed with the performance of the ACDs. They are interested in conducting further tests on our ACDs.

1. Ozioma Udochukwu Akakuru, Leonardo Martin-Alarcon, Steven Bryant, and Milana Trifkovic (2024) “Unravelling Water-Based Lubrication with Carbon Dots of Asphaltenes Origin”, Applied Materials & Interfaces, Accepted.

A provisional patent disclosure has already been filed in June 2023

2. Milana Trifkovic, Steven Bryant, Ozioma Akakuru (2023) “Composition for and method of making ratiometric sensing nanoparticle”, Provisional patent, application number #63472995.

H. BENEFITS

Please provide a narrative outline the project's benefits. Please use the subheadings of Economic, Environmental, Social and Building Innovation Capacity.

- **Economic:** Describe the project's economic benefits such as job creation, sales, improved efficiencies, development of new commercial opportunities or economic sectors, attraction of new investment, and increased exports.
- **Environmental:** Describe the project's contribution to reducing GHG emissions (direct or indirect) and improving environmental systems (atmospheric, terrestrial, aquatic, biotic, etc.) compared to the industry benchmark. Discuss benefits, impacts and/or trade-offs.
- **Social:** Describe the project's social benefits such as augmentation of recreational value, safeguarded investments, strengthened stakeholder involvement, and entrepreneurship opportunities of value for the province.
- **Building Innovation Capacity:** Describe the project's contribution to the training of highly qualified and skilled personnel (HQSP) in Alberta, their retention, and the attraction of HQSP from outside the province. Discuss the research infrastructure used or developed to complete the project.

RESPOND BELOW

Economic:

This project would lead to a positive impact on health and social well-being by creating a cleaner environment, and a stable economy that is less dependent on revenue from oil exports. The IP we already filed boosts clean technology, our plans to incorporate a company to aid commercialization of ACDs will create sustainable jobs, and the sale of ACDs as lubricant additives will surely grow the economy of Alberta.

Environmental:

This project developed a technology that converts asphaltenes to value-added materials (ACDs), which reduces the amount of bitumen sent for fuel refining and corresponding greenhouse gas emissions. Additionally, one of the applications we discovered for the ACDs is water-based lubricant additive. Traditional lubricants usually utilize petroleum-based oils and there are environmental challenges with disposal of used petroleum-based lubricants. As ACDs are hydrophilic, they tend to reduce this environmental problem.

Social:

Developing a viable method for producing low-cost ACDs is of high commercial interest, which requires establishing partnerships between us and lubricants/additives companies, and the global recognition and publicity that can spring up from such an achievement would put Alberta and its research institutions at

the leading edge of the technology. As cancer is one of the leading causes of death globally, the cancer imaging and therapeutic aspect of this project helps to improve public health.

Building innovation capacity:

This project trained 3 postdoctoral researchers, one master's degree student, and one undergraduate intern, all domiciled at the University of Calgary, Alberta. Strong plans are on the ground to incorporate a company for the commercialization of the project and are spearheaded by the HQSPs trained from the project, leading to their retention in Alberta. Part of the applications of the ACDs (thermal conductivity enhancement) was conducted in collaboration with researchers from another province of Canada (Toronto). We therefore believe that this project trained HQSPs, attracted HQSP from outside the province and has the capacity to retain them.

I. RECOMMENDATIONS AND NEXT STEPS

Please provide a narrative outlining the next steps and recommendations for further development of the technology developed or knowledge generated from this project. If appropriate, include a description of potential follow-up projects. Please consider the following in the narrative:

- Describe the long-term plan for commercialization of the technology developed or implementation of the knowledge generated.
- Based on the project learnings, describe the related actions to be undertaken over the next two years to continue advancing the innovation.
- Describe the potential partnerships being developed to advance the development and learnings from this project.

RESPOND BELOW

As regards commercialization of the technology, a provisional patent has already been filed. We are looking to successfully incorporate a company to enable commercialization of the product. We can currently produce 20 g per batch of ACDs in our lab. We are working towards developing a prototype to scale up production to 10 kg per batch. The estimated cost for setting up this prototype is approximately $100,000, leveraging the straightforward synthesis process of ACDs, mainly to cover the infrastructure cost. Concurrently, we are actively pursuing the establishment of connections and material transfer agreements with major oil sands producers to increase our asphaltenes supply chain. We hope to advance the technology to utilize liquid-state asphaltenes which will drastically reduce reliance on processed asphaltenes and attendant cost of the final product (ACDs).

We will be actively seeking funding for scaleup of this process.

Over the next two years, various actions will be taken to continue advancing the technology herein developed. We are looking into generating ACDs with liquid-state asphaltenes to reduce our reliance on solid-state asphaltenes. This will widen our supply chain and enhance the robustness of the technology. The ACDs developed in this technology are highly hydrophilic and as such they are very miscible with various materials. In this regard, we will continue to develop other applications based on nanocomposites of the ACDs. Apart from those already presented in this report about holographic sensing with ACDs/PVA nanocomposite, we have discovered substantial friction reduction with ACDs/polyethylene oxide composite.

As regards the partnerships being developed to advance the learnings from this project, we are actively pursuing customer validation which will be substantiated through successful contacts with industry leaders. A United Kingdom-based company specializing in lubricant additives, has expressed keen interest in deploying ACDs as a new type of lubricant additive, exploring non-aqueous additive formulations, and investigating their potential to reduce vehicle tailpipe emissions. Another company based in Canada, is interested in utilizing ACDs as additives for roof coatings, 2K floor coatings, and general coating additives. These established customer validations, along with ongoing explorations in different sectors, will accelerate the development cycle of ACDs and foster market penetration in the additives sector. Samples of the ACDs have already been sent out to one of these companies for exploration in their factory. The success of this trial will open new or improved applications for the ACDs.

J. KNOWLEDGE DISSEMINATION

Please provide a narrative outlining how the knowledge gained from the project was or will be disseminated and the impact it may have on the industry.

RESPOND BELOW

Bearing intellectual property protection in mind, peripheral aspects of the project have been presented at the (1) Calgary Innovation Fair, (2) Alberta Quantum Summit, (3) Canadian Chemical Engineering Conference, and (4) Alberta Biomedical Engineering Conference. The first three presentations were oral, while the last was a poster and did not require either submission or publication of abstracts. Industrialists and researchers discussed with us various aspects of the project, with particular emphasis on the biomedical aspect. We noticed that they have great enthusiasm to eventually see an asphaltene-derived material landing in the biomed world. Another interesting aspect of the discussions was the hydrophilicity of the ACDs, which is above par. One manuscript has already been accepted for publication based on the water-based friction reduction studies. Two other research manuscripts on tumor MRI and tumor photothermal imaging/therapy with the ACDs are ready for submission. A review article on

converting asphaltenes to high-value materials is also ready for submission. Two letters of support have been successfully obtained from two companies who are impressed with the performance of the ACDs and have shown interest in conducting further tests on our ACDs. A provisional disclosure has already been filed in June 2023. We therefore believe that our knowledge dissemination through the conference presentations and potential journal publications will adequately inform the biomed, hydraulic fracking and lubricants industries about a viable technological advancement with asphaltenes-bases materials.

K. CONCLUSIONS

Please provide a narrative outlining the project conclusions.

- Ensure this summarizes the project objective, key components, results, learnings, outcomes, benefits and next steps.

RESPOND BELOW

We successfully synthesized ACDs from asphaltenes for tumor imaging and therapy, metal-ion detection, friction reduction, thermal conductivity enhancement, and oil-water emulsion stabilization. Solvent pretreatment of the asphaltenes precursor was utilized in this technology for the first time as a strategy to boost the reactivity of asphaltenes for oxidation reaction to ACDs and asphaltene oxide. Our facile and rational synthesis route enables the generation of indistinguishable ACDs and asphaltene oxide from various asphaltene sources, thus side-stepping the challenge of source-dependent asphaltenes variation. This variation has been a bottleneck in asphaltenes technological development. The ACDs and asphaltene oxide were extensively characterized to determine their morphology as nano disc-shaped nanomaterials. Whereas the size of the ACDs is below 15 nm, typical of carbon dots, the size of asphaltene oxide ranges from 30-90 nm. The size of the asphaltene oxide could easily be tuned by varying the reaction temperature. Thermogravimetric analysis shows that the ACDs and asphaltene oxide are relatively stable up to 600^{o}C, suggesting their capability for deployment in systems that operate at high temperature. Both ACDs and asphaltene oxide possess abundant oxygen- and nitrogen-containing groups that endow them with excellent water re-dispersibility even after oven drying. Raman spectroscopy reveals that the ACDs and asphaltene oxide possess more defect-band than graphitic band, confirming the presence of abundant oxygen- and nitrogen-containing groups in their structure. These functional groups account for the high negative zeta potential (surface charge) of the ACDs and asphaltene oxide.

The functional groups in the ACDs were leveraged to complex metal ions such as iron and manganese to prepare ACD-metal ion complexes that could serve as contrast agents for magnetic resonance imaging (MRI). This could enable the use of the ACDs as a component of hydraulic fracking fluid for sensing oil deposits underground using the MRI modality. The ACDs alone were established as photothermal agents which could convert near infrared light to heat to cause tumor death in vivo. We discovered that tumor

regression could be achieved within 15 days post-injection of the ACDs into tumor-bearing mice following tumor photothermal therapy. Simultaneously, the tumor region could be imaged with the ACDs by photothermal imaging technique. When complexed with iron, ACD-iron complexed was successfully used for tumor imaging by MRI. The ACDs were also established to be biocompatible suggesting their suitability for biomedical application.

Furthermore, the ACDs were used to prepare water-based lubricants for friction reduction, where they were recorded to reduce friction between steel-steel surfaces by 54%. This suggests the potential use of the ACDs as an alternative to petroleum-based lubricants which have environmental concerns and resource scarcity challenges. The friction-reduction performance of the ACDs outperformed those of most pristine carbon dots, graphene quantum dots, graphene oxide, and commercial nanomaterials such as 5 and 20 nm silica nanoparticles. Both ACDs and asphaltene oxide were established to enhance thermal conductivity of water, ethylene glycol, and antifreezes (using car radiator coolant as a model). The asphaltene oxide could enhance the thermal conductivity of car radiator coolant by 20% at room temperature. The ACDs alone could adequately stabilize regular oil-water emulsion, including high interface Pickering emulsions (HIPEs) that usually possess high oil fraction. The lowest loading of stabilizers that have been reported for stabilizing HIPEs is achieved with the ACDs. The ACDs-stabilized HIPEs thus possesses flowable properties that enable using the emulsions in 3D printing of different shapes. The beneficial surface functionality of the ACDs described above endows the ACDs with easy miscibility with various compounds. This was exemplified when the ACDs were mixed with poly vinyl alcohol and used as a to construct a holographic sensing material.

The various applications of ACDs uncovered in this project shine light into the possibility of deploying asphaltenes-based materials in different fields. It is expected that these discoveries will spur more research into asphaltenes technological development to foster the conversion of asphaltenes to high-value materials. The benefits of this project are far reaching. Considering that different highly qualified and skilled personnel were trained in this project within Alberta and beyond and the plan to incorporate a company for the commercialization of the ACDs, this project has substantial economic impact alongside building innovation capacity. By reducing the amount of bitumen sent for fuel refining plus the energy requirement during the refining process, this project which uses the asphaltenes directly to generate high-value materials for meaningful applications contributes significantly to reducing greenhouse gasses towards net zero carbon emissions. During this project duration, connections have been established with various industries in Canada and outside, which ultimately add to the societal benefits of Alberta. The next plan for this project will be to scale up our current production scale from 10 g per day to 10 kg per day. This will require the development of a prototype for mass production, funding, and harmonizing our asphaltenes supply chain.